Multifunctional light-field modulation based on hybrid nonlinear metasurfaces

Shuhang Qian(钱树航), Kai Wang(王凯), Jiaxing Yang(杨加兴), Chao Guan(关超),Hua Long(龙华), and Peixiang Lu(陆培祥)

Citation: Chin. Phys. B, 2023, 32 (**10**): 107803. DOI: 10.1088/1674-1056/acdc13

Journal homepage: http://cpb.iphy.ac.cn; http://iopscience.iop.org/cpb

What follows is a list of articles you may be interested in

Probing photocarrier dynamics of pressurized graphene using time-resolved terahertz spectroscopy

Yunfeng Wang(王云峰), Shujuan Xu(许淑娟), Jin Yang(杨金), and Fuhai Su(苏付海)

Chin. Phys. B, 2023, 32 (**6**): 067802. DOI: 10.1088/1674-1056/acc2b1

Signal-to-noise ratio of Raman signal measured by multichannel detectors

Xue-Lu Liu(刘雪璐), Yu-Chen Leng(冷宇辰), Miao-Ling Lin(林妙玲), Xin Cong(从鑫), and Ping-Heng Tan(谭平恒)

Chin. Phys. B, 2021, 30 (**9**): 097807. DOI: 10.1088/1674-1056/ac1f06

Thermally induced band hybridization in bilayer-bilayer MoS_2/WS_2 heterostructure

Yanchong Zhao(赵岩翀), Tao Bo(薄涛), Luojun Du(杜罗军), Jinpeng Tian(田金朋), Xiaomei Li(李晓梅), Kenji Watanabe, Takashi Taniguchi, Rong Yang(杨蓉), Dongxia Shi(时东霞), Sheng Meng(孟胜), Wei Yang(杨威), and Guangyu Zhang(张广宇)

Chin. Phys. B, 2021, 30 (**5**): 057801. DOI: 10.1088/1674-1056/abeee3

Modulation of the second-harmonic generation in MoS_2 by graphene covering

Chunchun Wu(吴春春), Nianze Shang(尚念泽), Zixun Zhao(赵子荀), Zhihong Zhang(张智宏), Jing Liang(梁晶), Chang Liu(刘畅), Yonggang Zuo(左勇刚), Mingchao Ding(丁铭超), Jinhuan Wang(王金焕), Hao Hong(洪浩), Jie Xiong(熊杰), and Kaihui Liu(刘开辉)

Chin. Phys. B, 2021, 30 (**2**): 027803. DOI: 10.1088/1674-1056/abd77f

Efficient doping modulation of monolayer WS_2 for optoelectronic applications

Xinli Ma(马新莉), Rongjie Zhang(张荣杰), Chunhua An(安春华), Sen Wu(吴森), Xiaodong Hu(胡晓东), Jing Liu(刘晶)

Chin. Phys. B, 2019, 28 (**3**): 037803. DOI: 10.1088/1674-1056/28/3/037803

REVIEW

Multifunctional light-field modulation based on hybrid nonlinear metasurfaces

Shuhang Qian(钱树航)[1], Kai Wang(王凯)[1,2,†], Jiaxing Yang(杨加兴)[1], Chao Guan(关超)[1], Hua Long(龙华)[1], and Peixiang Lu(陆培祥)[1,3]

[1] *Wuhan National Laboratory for Optoelectronics and School of Physics, Huazhong University of Science and Technology, Wuhan* 430074, *China*
[2] *School of Electronic and Information Engineering, Hubei University of Science and Technology, Xianning* 437100, *China*
[3] *Hubei Key Laboratory of Optical Information and Pattern Recognition, Wuhan Institute of Technology, Wuhan* 430205, *China*

(Received 6 May 2023; revised manuscript received 6 June 2023; accepted manuscript online 7 June 2023)

The generation characteristics of nonlinear optical signals and their multi-dimensional modulation at micro-nano scale have become a prominent research area in nanophotonics, and also the key to developing various novel nonlinear photonics devices. In recent years, the demand for higher nonlinear conversion efficiency and device integration has led to the rapid progress of hybrid nonlinear metasurfaces composed of nanostructures and nonlinear materials. As a joint platform of stable wavefront modulation, nonlinear metasurface and efficient frequency conversion, hybrid nonlinear metasurfaces offer a splendid opportunity for developing the next-generation of multipurpose flat-optics devices. This article provides a comprehensive review of recent advances in hybrid nonlinear metasurfaces for light-field modulation. The advantages of hybrid systems are discussed from the perspectives of multifunctional light-field modulation, valleytronic modulation, and quantum technologies. Finally, the remaining challenges of hybrid metasurfaces are summarized and future developments are also prospected.

Keywords: light-field modulation, hybrid metasurfaces, nonlinear optics, two-dimensional materials

PACS: 78.67.Pt, 81.05.Xj, 42.65.–k, 78.67.–n **DOI:** 10.1088/1674-1056/acdc13

1. Introduction

With the flourishing development of micro-nano optoelectronic devices, the conventional optical components are unsuitable for contemporary integrated and miniaturized optoelectronic systems due to their large size and limitations imposed by micro-nano manufacturing technologies. The proposal of metasurfaces has unveiled a new avenue for the design of optical elements, facilitating the manipulation of light in ways beyond the reach of natural materials.[1–3] The effective control of polarization, amplitude and phase of light at subwavelength scales is achievable by introducing an abrupt change in phase to two-dimensional (2D) or quasi-two-dimensional metasurfaces made of metallic or dielectric materials.[4–10] The first proposal of generalized Snell's Law demonstrated the capability of phase-discontinuous metasurfaces to manipulate light in unconventional ways,[5] leading to a variety of metasurfaces using P–B phase and resonant phase modulation exhibiting numerous intriguing functions in the field of linear optics,[11–23] including beam focusing and metalens,[13,24–27] optical holography,[28–34] versatile polarization generation,[35] and vortex beam generation and manipulation.[18,36–39] The emergence of metasurfaces heralds the era of planar optics.

Nonlinear optics has been a thriving research field over the past several decades.[40] The second harmonic generation (SHG), third harmonic generation (THG), and photoinduced refractive index variation have extensive applications in frequency conversion, all-optical switching, and electro-optical switching.[41–44] Traditional nonlinear optical crystals have achieved great success in laser frequency conversion. However, the rapid advancement of optical computing and quantum optical chips has made the integration of nonlinear optics into micro-nano sized chips an imperative scientific and technological challenge. In recent years, the emergence of nonlinear metasurfaces has provided marvellous opportunities for designing and implementing nonlinear optical elements with specific functions in light-field modulation.[45–47] The integration of nonlinear optical effects endows light-field modulation with new controllable degrees of freedom such as frequency, amplitude, phase, and polarization. This enables the multi-dimensional modulations of the light field while producing a nonlinear signal, greatly reducing the size and footprint of the optoelectronic system. Owing to its broadband tunability, a single metasurface can carry multiple information channels, significantly enriching the functionality of the micro-nano optical devices.

Nevertheless, despite the benefits offered by the amalgamation of nonlinear optical effects, conventional nonlinear metasurfaces are encountering new challenges in keeping up with the increasing demand for high nonlinear conversion effi-

[†]Corresponding author. E-mail: kale_wong@hust.edu.cn

ciency and stable performance of wavefront manipulation. In the field of nonlinear light-field modulation, nonlinear metasurfaces are required to act not only as efficient nonlinear signal generators but also to modulate the phase of nonlinear signals at the subwavelength scale. On the one hand, while dielectric metasurfaces have the capability to produce strong electromagnetic field enhancement, the complex electromagnetic resonance modes make it challenging to create independent phase modulation units. Additionally, the local electric field generated by the dielectric meta-atoms is susceptible to being affected by neighboring meta-atoms,[48] resulting in decreased phase modulation capabilities compared to plasmonic metasurfaces. On the other hand, metal materials often exhibit large ohmic losses and low damage thresholds, and strong absorption caused by resonance can lead to damage of the metal structure due to accumulated thermal effects, especially in the visible band. Additionally, when the power of the pump laser is high, interference from high-order nonlinear signals like supercontinuum light may be generated.[49,50] One potential solution to the dilemmas aforementioned is to amalgamate the advantages of plasmonic and dielectric metasurfaces with nonlinear materials to create hybrid nonlinear metasurfaces. The hybrid nonlinear metasurfaces generally refer to metasurfaces that combine conventional metasurfaces with other materials or nanostructures, resulting in metasurfaces containing more than one type of material. In virtue of the high nonlinear conversion efficiency, stable capability of phase modulation, and ease of integration, hybrid nonlinear metasurfaces have become promising candidates for multifunctional nonlinear micro-nano devices.

Herein, we will provide a general overview of the latest research progress related to hybrid nonlinear metasurfaces. This paper is mainly divided into four parts. In the second part, we will briefly introduce the functions that conventional nonlinear metasurfaces have achieved in light-field modulation, including plasmonic and dielectric metasurfaces. In the third part, we will discuss the novel and feature-rich hybrid nonlinear metasurfaces in detail, including their applications in nonlinear phase modulation, nonlinearity enhancement, valleytronic modulation and quantum technologies. Finally, we will provide a conclusion and make an outlook on future research in hybrid nonlinear metasurfaces.

2. Conventional nonlinear metasurfaces

2.1. Plasmonic nonlinear metasurfaces

The two typical metal nanostructures for nonlinear phase modulation are the U-shaped split-ring resonators (SRRs) and the Y-shaped nanoantennas with three-fold ($C3$) rotational symmetry.[46,51–69] SRRs exhibit an electromagnetic response over a wide range of wavelengths. U-shaped plasmonic nanorods generate a ring-shaped surface plasmon current, resulting in both electrical and magnetic coupling, which grants them remarkable ability in light-field modulation. The SHG of U-shaped SRRs has been studied since 2012.[54] Afterwards, the wavefront manipulation of SHG was realized by introducing phase mutation by flipping the U-shaped SRR unit.[55] Subsequently, based on the same approach, the generation of second-harmonic Airy beams and vortex beams was also demonstrated.[56] Furthermore, P–B phase modulation can be introduced to SRRs with different rotation angles. Under the excitation of circularly polarized light, photons with different frequencies will carry distinct phase factors, which endow a single metasurface with multiple information channels.[58–60] Figure 1(a) shows a gradient nonlinear metasurface with U-shaped nanopores that rotate to generate a spin-selective second harmonic vortex beam.[60] In addition, SRRs also exhibit a chiral response to circularly polarized light by changing the incident angle, which extends the functionality of metasurfaces in another dimension.[61]

Based on similar principles, Y-shaped nanoantennas with $C3$ symmetry can also realize various phase modulation functions. As shown in Fig. 1(b), a nonlinear metalens imaging system that integrates ultra-thin planar lenses with synchronous frequency conversion function has been demonstrated.[64] By introducing the focusing phase into the metasurface, an L-shaped object in the near-infrared band was imaged in the visible range of the second-harmonic signal. Additionally, Y-shaped nanorods based on P–B phase modulation can also achieve optical image encoding,[65] making them suitable as optical encryption devices. Building upon this capability, the far-field holographic imaging was also achieved by combining amplitude and phase modulation of SHG.[67] Figure 1(c) shows a method for nonlinear vectorial holography based on geometric phase metasurface.[69] The amplitude and phase of the left-handed and right-handed circular polarized (LCP and RCP) SHG can be modulated respectively by controlling the rotation angles of the four meta-atoms in the metasurface. And through the combination of holographic calculation and reverse design methods, SH holographic images with arbitrary polarization distributions can be generated. Similarly, such plasmonic nanorods with specific symmetry can also be employed for SH vortex beam generation[63] and THG manipulation.[46]

Moreover, nonlinear metasurfaces also have essential applications in the THz band.[53,70] Figure 1(d) shows a nonlinear metalens based on the Fresnel zone plate, which can generate broadband terahertz radiation and selectively focus its different frequency components along the optical axis simultaneously. The demonstration of controllable emission and focusing of terahertz waves opens up an avenue for creating various metasurface-based terahertz emitters, and is expected to

develop efficient, integrated, and ultra-compact optical devices in the terahertz spectral region.

In general, the electromagnetic resonance modes in the plasmonic metasurfaces are uncomplicated, resulting in superior phase modulation ability compared with the dielectric metasurfaces, and thus easier to realize various light-field modulation functions. However, there are also several obvious drawbacks in the plasmonic metasurfaces, such as large ohmic losses and low damage thresholds. It is liable to cause structural damage under high-power excitation, which greatly limits the excitation power and puts an inherent upper limit on the nonlinear conversion efficiency of plasmonic metasurfaces due to the nonlinear conversion efficiency depends heavily on the power density of excitation light. Therefore, the plasmonic metasurfaces still have limitations in practical applications compared to dielectric metasurfaces.

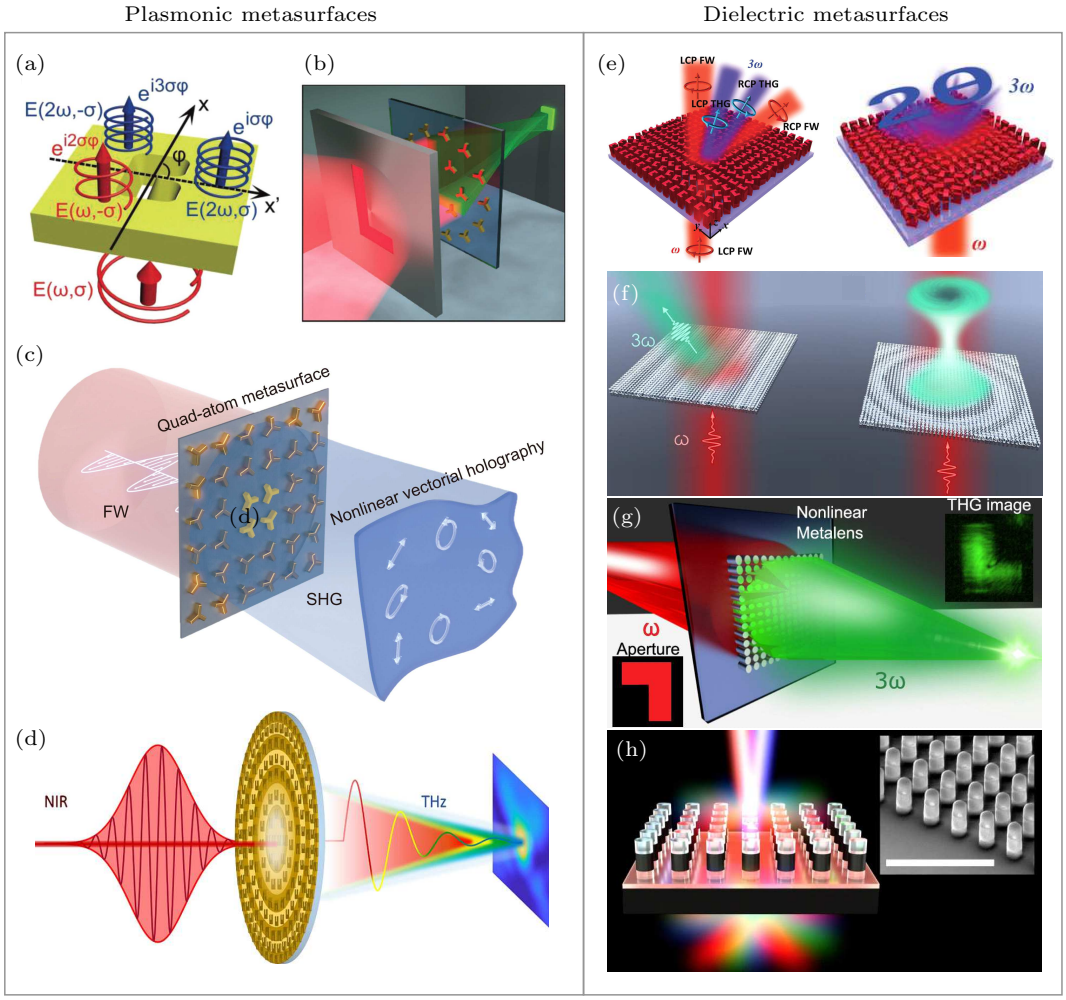

Fig. 1. (a) Schematic of multi-channel wavefront manipulation by introducing P–B phase on U-shaped nanopore metasurface.[60] (b) Schematic of nonlinear imaging using metalens composed of *C*3 nanoantennas.[64] (c) Schematic of P–B phase metasurface for nonlinear vectorial holography.[69] (d) Schematic of controllable emission and manipulation of THz waves using a Fresnel zone plate based metasurface.[53] (e) Schematic of THG manipulation of P–B phase metasurface composed of Si nanopillars.[78] Left panel: nonlinear beam deflection. Right panel: nonlinear holography. (f) Schematic of multifunctional nonlinear metasurface composed of silicon elliptical nanopillars for nonlinear beam deflection and generation of nonlinear focusing vortex beam.[71] (g) Schematic of the third-harmonic metalens imaging. The insets in the lower left and upper right corners are L-shaped apertures and their corresponding third-harmonic images, respectively.[77] (h) Schematic of nonlinear optical frequency mixer based on GaAs metasurface. Various new frequencies are concurrently generated after pumping by two femtosecond near-infrared pulses. Inset: scanning electron microscope (SEM) image of the GaAs meta-atoms, the scale bar is 3 μm.[75]

2.2. Dielectric nonlinear metasurfaces

Dielectric materials are also extensively employed in light-field modulation.[71–80] Compared to plasmonic metasurfaces that rely on surface plasmons, dielectric metasurfaces utilize local resonance of the electric field within the nanoresonator, resulting in a larger area of nonlinearity than metal particles. Therefore, it is well-suited for studying higher-order nonlinear effects. Currently, silicon is one of the most prevalent dielectric materials utilized in light-field modulation. Due to its excellent refractive index and third-order nonlinear coefficient, numerous investigations have focused on designing dielectric metasurfaces using silicon as a carrier to manipulate THG. Figure 1(e) depicts the utilization of Si nanopillars with varying rotation angles to introduce the P–B phase, leading to beam steering and holographic imaging of THG.[78]

Besides the P–B phase, resonant phase modulation is

a more commonly used technique in all-dielectric nonlinear metasurfaces. For the dielectric nanostructures, when the driving frequency deviates from the intrinsic frequency of the electronic vibration in the structure, the electronic vibration will lead to changes in both amplitude and phase. Therefore, by modifying the shape of the nanostructure, the phase and amplitude of the emitted light field can be modulated. As shown in Fig. 1(f), the phase modulation of the THG signal is achieved by altering the size of the silicon elliptical nanopillars, beam deflection, focusing, and nonlinear vortex beam generation are demonstrated.[71] Based on similar principles, dual-resonant high-efficiency third-harmonic holographic imaging has also been achieved.[72] In addition, dielectric metasurfaces based on resonant phase modulation can also enable nonlinear metalens imaging,[77] as shown in Fig. 1(g). With appropriate design, giant localized electromagnetic fields can be formed inside the dielectric nanostructures thereby enhancing the generation of nonlinear signals. Figure 1(h) shows a nonlinear optical frequency mixer based on GaAs metasurfaces.[75] Due to the intrinsic even- and odd-order nonlinearity of GaAs materials, enhanced electromagnetic fields and relaxed phase matching requirements, this metasurface can concurrently generate eleven new frequencies spanning from ultraviolet to near-infrared regions.

In addition, dielectric metasurfaces can also support other resonant modes with high quality factor (Q-factor). For instance, Mie-resonance,[81] anapole resonator,[82–84] and resonance induced by quasi-bound states in the continuum (quasi-BIC).[85–88] The efficiency of nonlinear signal generation in quasi-BIC resonant metasurfaces is highly influenced by the Q-factor of the electromagnetic resonance mode in the structure.[89] Currently, quasi-BIC resonant metasurfaces have demonstrated the highest THG conversion efficiency.[90,91] Furthermore, dielectric metasurfaces have shown potential for higher-order harmonic generation.[92,93] In 2018, Liu *et al*. reported the generation of higher-order harmonics in all-dielectric metasurface.[92] As a result of intense Fano-resonance supported by Si metasurface, odd-order harmonics up to 11th order can be measured.

Overall, dielectric metasurfaces offer a high damage threshold and strong local field enhancement, making them a compelling platform for generating and manipulating nonlinear signals and other strong field processes at the nanoscale.

3. Hybrid metasurfaces

As mentioned previously, the concept of metasurfaces has expanded into the field of nonlinear optics, enabling complete control of the wavefront of nonlinear beams. The proposal of hybrid nonlinear metasurfaces has attracted extensive interest, and promoted the exploration and research on nonlinear materials. We have summarized typical nonlinear optical processes (e.g., SHG, THG) in various commonly used nonlinear materials and their key parameters (e.g., $\chi^{(2)}$, $\chi^{(3)}$, emission wavelength, and refractive index) in Table 1. Under appropriate excitation conditions, the second-order susceptibility of transition metal dichalcogenides (TMDCs) can reach tens or even hundreds of nm/V, and they also exhibit third-order nonlinear characteristics. In the following sections, we will discuss the diverse nonlinear light-field modulation functions of hybrid metasurfaces based on these nonlinear materials.

Table 1. Basic nonlinear optical properties of commonly used nonlinear materials. For SHG, $\chi^{(n)}$ represents $\chi^{(2)}$, in nm/V; for THG, $\chi^{(n)}$ represents $\chi^{(3)}$, in nm^2/V^2. The column with the mark – means that the value is already listed in other columns.

	Materials	$\chi^{(n)}$	Emission wavelength (nm)	Refractive index
SHG	WS_2	9;[94]	415;[94]	2.72–5.90
		0.68[95]	560–665[95]	(400 nm–850 nm)[96]
	MoS_2	5, 100;[97]	405;[97,98]	0.89–4.31
		32[98]	780[99]	(190 nm–1700 nm)[100]
		0.029[99]		
	WSe_2	60;[101]	700–800;[101]	2.72–5.55
		10[102]	408[102]	(400 nm–850 nm)[96]
	$MoSe_2$	0.01–0.05[103]	600–900[103]	3.25–5.73
				(400 nm–850 nm)[96]
	ZnO	0.0014–0.014[104]	532[104]	1.89–2.10
				(450 nm–4000 nm)[105]
	GaAs	0.24, 0.34[106]	532, 766[106]	3.43–5.04
				(260 nm–1880 nm)[107]
	$LiNbO_3$	0.0096–0.0514[106]	426[106]	2.05–2.44
				(400 nm–5000 nm)[108]
THG	WS_2	0.24[109]	520[109]	–
	MoS_2	0.24;[99]	520;[99]	–
		0.05–0.21[110]	586–660[110]	
	WSe_2	0.1[109]	520[109]	–
	$MoSe_2$	0.22[109]	520[109]	–
	graphene	40;[111]	575;[111]	1.49–3.02
		0.25–1.2[112]	433–550[112]	(250 nm–1000 nm)[113]
	ZnO	0.03[114]	500[114]	–
	Si	0.135–0.245[115]	517–1420[115]	1.67–3.49
				(250 nm–1450 nm)[116]

3.1. Phase modulation

In recent years, the 2D materials represented by TMDCs have drawn considerable attention. Monolayer TMDCs with an atomic layer thickness not only exhibit outstanding nonlinear properties ($\chi^{(2)}$ is about nm/V even under a thickness of less than 1 nm),[117–120] but also can be effortlessly integrated into optical nanostructures.[121–127] Due to the relaxed phase matching constraints of 2D materials resulting from their ultrathin thickness,[117–120] plasmonic-2D materials hybrid metasurfaces have been proposed as a novel and promising solution for achieving higher-efficiency nonlinear light-field modulation.

The principle of phase modulation in plasmonic-2D mate-

rials hybrid metasurfaces can be briefly illustrated in Fig. 2(a). For a hybrid system consisting of Au nanoholes metasurface and monolayer WS_2, the incident circularly polarized fundamental wave is initially applied to the metasurface for P–B phase modulation. As a result, half of the transmitted circularly polarized light carries an additional P–B phase factor of 2θ and is opposite to the polarization states of the incident light, where θ is the rotation angle of the meta-atom. Then the fundamental wave with a phase factor of 2θ is further pumped onto the WS_2 to generate second harmonics. Since the SHG process of monolayer WS_2 needs to comply with the specific selection rules,[101,128] the polarization state of second harmonics generated by the fundamental wave carrying P–B phase factor excited WS_2 will be reversed, and the corresponding P–B phase factor will become 4θ.[129] Therefore, the efficient nonlinear signal generation and stable phase modulation can be achieved by designing the metasurface phase plate through backward derivation, which is also convenient even for the higher-order nonlinear signals.

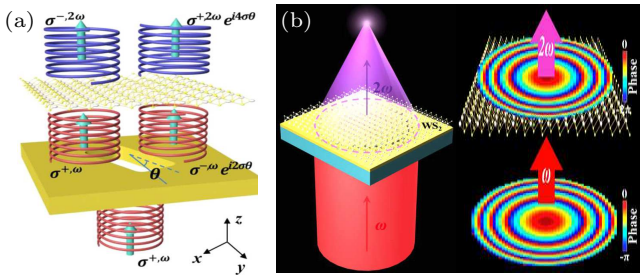

Fig. 2. (a) Schematic illustration of the principle of SH phase modulation in the WS_2–Au nanoholes hybrid metasurface.[129] (b) Schematic of SHG focusing on a nonlinear metalens based on the WS_2–Au nanoholes hybrid metasurface (left panel). In the right panel, from bottom to top, are the phase distribution of the fundamental wave passed through the gold nanoholes and the transmitted SHG signal, respectively.[130]

Based on this mechanism, a high-efficiency second-harmonic metalens is implemented, as shown in Fig. 2(b). The WS_2 monolayer is transferred intact to the gold nanoholes array to form a hybrid metasurface, resulting in the focusing of the SHG signal in the emission direction.[130] The gold nanoholes array acts as a phase modulation plate for the fundamental wave by introducing the P–B phase, while the monolayer WS_2 acts as an efficient second-harmonic emitter. And this hybrid metasurface exhibits a large second-order susceptibility, approximately 0.1 nm/V at a wavelength of 810 nm, which is 2–3 orders of magnitude greater than that of conventional plasmonic metasurfaces. In addition, this 2D material-based hybrid metasurface is capable of integrating functions such as polarization control, beam steering, and vortex beam generation simultaneously.[131] These works provide new ideas for the design of nonlinear metasurfaces.

Subsequently, researchers have conducted various studies on nonlinear light-field modulation using the plasmonic-2D materials hybrid metasurfaces. Figure 3(a) shows a method for controlling the in-plane nonlinear polarization phase of TMDCs.[132] Coupling a monolayer MoS_2 to a plasmonic phased array antenna and adjusting the phase delay between the two primary axes of the antenna elements to manipulate the direction of SH emission. Similarly, flexible manipulation of SHG can also be achieved through nanophotonic gratings,[133] as shown in Fig. 3(b). Researchers have also applied the polarization conversion process of SHG in the hybrid metasurface mentioned above to SHG imaging, which indicates the great potential of hybrid nonlinear metasurfaces in controlling the polarization states and optical chirality.[134] Figure 3(c) presents a scheme for generating chiral SHG using plasmonic vortex metalens.[135] This approach involves transferring WS_2 onto a spiral slit on the surface of an aluminum film and utilizing the enhanced effect of a plasmonic vortex field under spin–orbit interaction, resulting in a giant SHG circular dichroism. This 2D spiral plasmonic structure is a universal method for generating near-field vortex fields with tunable topological charges.

The versatility demonstrated by hybrid nonlinear metasurfaces offers the potential for full optical generation of vortex beams. Nonlinear vortex beams possess a helical wavefront phase at the harmonic frequency, providing an additional degree of freedom. The wavelength of the n-th harmonic signal is exactly $1/n$ of the fundamental wavelength, which geometrically improves the capabilities of communication and information encoding. In 2021, the generation of SH vortex beams with large topological charges (up to 28) based on Au–WS_2 hybrid metasurface was experimentally demonstrated.[129] To optimize imaging quality and avoid the dissipation of the SH vortex beam during free space propagation, a focusing phase is added. The doughnut-shaped light field distribution can be clearly observed at a focal length of 50 μm, as shown in Fig. 3(d). This result may open up new avenues for generating harmonic optical vortices in optical communication.

The manipulation of nonlinear wavefronts by hybrid metasurfaces has not only brought a series of breakthroughs but also opened up a new field of vision, leading to the development of nonlinear computational holography technologies. Metasurface holography is an imaging technique that involves the calculation and inversion of the phase information of a desired object, followed by the use of a metasurface to create a corresponding phase plate to reconstruct the object image. Nonlinear computational holography is a promising method for encoding and processing information due to its excellent capacity to carry and edit large amounts of information. However, it also places higher demands on the nonlinear conversion efficiency and wavefront manipulation performance, which is

quite challenging. In 2020, the chirality-selected SH holography using a WS_2–Au hybrid metasurface was reported,[136] as shown in Fig. 3(e). In this study, binary amplitude modulation was introduced into the gold metasurface, resulting in an improvement in both the average intensity and the imaging quality of the hologram. Subsequently, a novel resonant hybrid nonlinear metasurface was proposed to achieve high-efficiency generation and amplitude-phase joint modulation of SHG.[137] As shown in Fig. 3(f), the metasurface consisted of a series of V-shaped gold nanoholes with different open angles, which were used to modulate the amplitude and phase of the fundamental wave. The experimental results indicated an improved imaging quality and signal-to-noise ratio compared to the pure phase modulation.

Hybrid nonlinear metasurfaces have wide applications not only in the visible region, but also in the microwave and terahertz (THz) regions. On the one hand, graphene has been applied to construct hybrid metasurfaces to control wavefront due to its robust plasmonic response in the microwave region.[138] As shown in Fig. 3(g), the phase modulation and far-field radiation pattern tuning can be realized through changing the voltage applied to graphene. On the other hand, functional devices based on graphene hybrid metasurfaces have also been demonstrated in the THz region, such as polarization converter, switchable wave deflection device, and dualpolarity tunable focusing mirror.[139] Figure 3(h) shows an electrically tunable graphene hybrid metasurface with the function of focusing terahertz energy.[140] The focal length of the metalens can be electrically tuned within a range of two millimeters, making it a promising candidate for terahertz imaging. In addition, low energy THz wave modulators based on graphene-dielectric hybrid metasurfaces have also been demonstrated,[141] providing a valuable reference for the design of dynamic light modulators and sensors in the THz region.

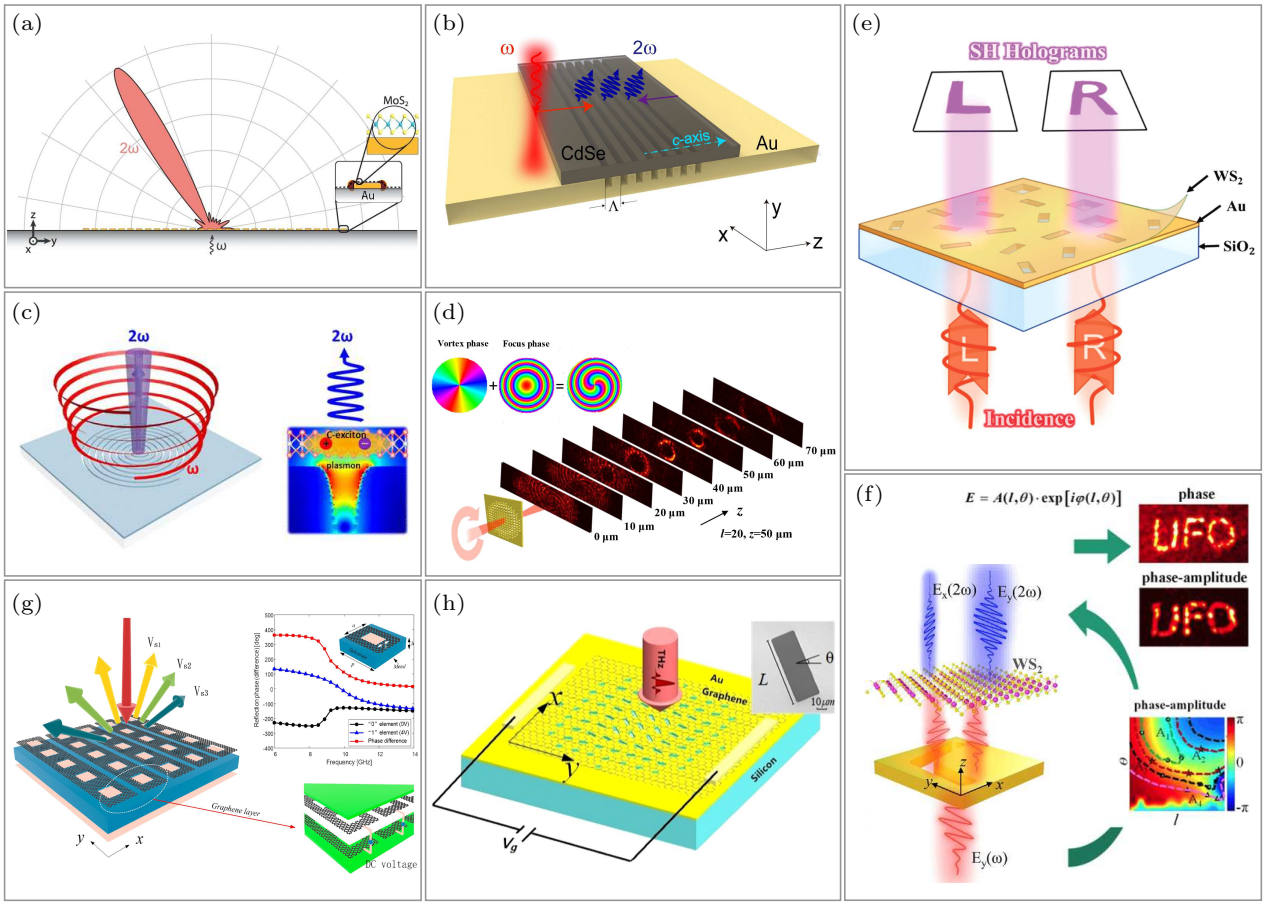

Fig. 3. (a) Schematic of MoS_2-plasmonic phased array antennas hybrid metasurface for SHG steering.[132] (b) Schematic of CdSe nanobelt–Al_2O_3–Au gratings hybrid metasurface for SHG steering.[133] (c) Schematic of chiral SHG from the aluminum plasmonic vortex lens (left panel). The simulated local field enhancement of aluminum nanoslit was designed at the C-exciton resonance of WS_2 (right panel).[135] (d) Experimentally measured propagation of the emitted SH vortex beam along the z-axis with 10 μm steps, the topological charges are 20, the focal plane at $z = 50$ μm. The inset in the upper left corner shows the phase distribution of the focus array, vortex array, and focus-vortex array, respectively.[129] (e) Schematic illustration of WS_2–Au nanoholes hybrid metasurface for chirality-selected SH holography.[136] (f) Illustration of the operational mechanism of resonant hybrid nonlinear metasurface. The desired y-polarized SHG is modulated under an excitation of a y-polarized incident laser at a wavelength of 810 nm.[137] (g) Schematic of microwave graphene hybrid metasurface (left panel). The detailed drawing of the graphene sandwich structure is shown in the lower right corner. The upper right corner shows the reflection phase of the meta-atom.[138] (h) Schematic of electrically tunable THz metalens composed of graphene and Au nanopores. The inset shows the SEM image of a single meta-atom.[140]

3.2. Nonlinearity enhancement

Improving the interaction between light and matter has always been the focus of nonlinear optical devices. In addition to the applications in phase modulation and beam manipulation, hybrid nonlinear metasurfaces based on 2D materials have also exhibited remarkable performance for nonlinearity enhancement.[142,143] Figure 4(a) shows the combination of monolayer WS_2 and Ag nanogratings, a 400-fold SHG enhancement is realized using surface plasmon resonant mode supported by Ag nanogratings.[144] Moreover, it also integrates the capability of controlling the polarization state of SHG.

Besides plasmonic metasurfaces, the combination of 2D materials with dielectric metasurfaces can also achieve tremendous nonlinear enhancement.[127,145] Figure 4(b) shows a hybrid metasurface composed of T-shaped silicon nanopillars coupled with a 2D GaSe flake. The high Q-factor and large mode area generated from the quasi-BIC supported by the metasurface are utilized to uniformly enhance the SHG of GaSe flake by nearly 4 orders of magnitude under continuous wave pumping.[146] This finding has the potential to advance the development of high-power coherent light sources. The hybrid metasurface based on Fabry–Pérot (F–P) microcavity can also yield a giant enhancement in nonlinear optical response.[126] By coupling a monolayer WS_2 with a SiO_2/Si hole array to form an F–P micro-cavity and tuning the pump wavelength to match the resonant mode of the micro-cavity, a SHG enhancement of approximately 1580 times is achieved, as depicted in Fig. 4(c).

In addition to the SHG enhancement, hybrid metasurfaces have also demonstrated efficacy in the sum-frequency generation (SFG).[147] As shown in Fig. 4(d), the second-order nonlinearity of GaSe flake can be augmented through Fano-resonance supported by silicon metasurface. Similarly, high-efficiency frequency mixing can also be realized by coupling a monolayer WS_2 with a dielectric photonic crystal (PC) waveguide, as shown in Fig. 4(e). The monolayer WS_2 served as an efficient nonlinear emitter and the counter-propagating Bloch surface waves are simultaneously launched via the grating couplers. By simultaneously lifting the spatiotemporal overlap of two counter-propagating Bloch surface waves and the nonlinear crystal, the efficient nonlinear frequency mixing will occur at the WS_2 region.[123] In addition to their potential for nonlinearity enhancement, hybrid metasurfaces have also shown promise in laser generation[148,149] and pulse shaping.[150] Figure 4(f) shows a novel scheme of hybrid metasurface to shape the temporary profile of a pulse.[150] The overall hybrid structure is composed of monolayer MoS_2 and TiO_2 nanorods located on a distributed Bragg reflector (DBR). Under normal incidence, the introduction of in-plane asymmetries induces a quasi-BIC resonance, and a variety of pulse shaping operations are realized upon enlarging the permittivity variation of MoS_2, including pulse compression, expansion, splitting and higher-order distortion.

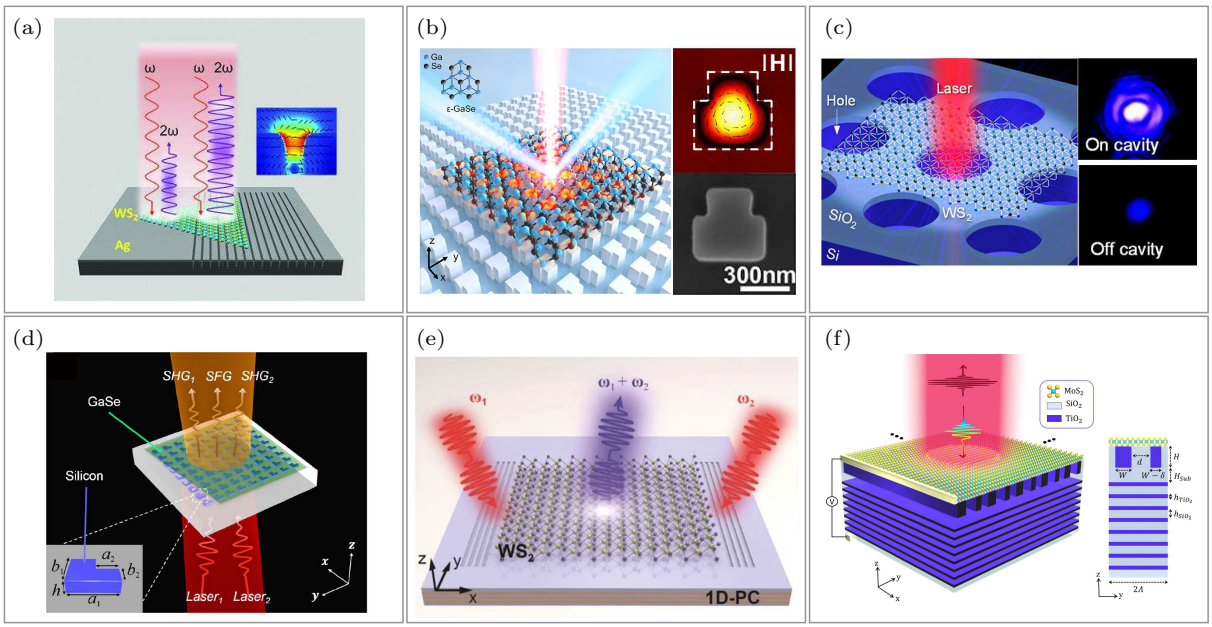

Fig. 4. (a) Schematic of WS_2–Ag nanogratings hybrid metasurface for SHG enhancement and polarization states to control. The inset shows simulated electric field distribution at a second-harmonic wavelength in the nanogroove.[144] (b) Schematic of GaSe–Si hybrid metasurface for SHG enhancement (left panel). The right panel shows simulated magnetic field distribution at quasi-BIC mode in the x–y plane (up) and an SEM image of a single T-shaped silicon nanopillar (bottom).[146] (c) Schematic of the hybrid metasurface based on F–P micro-cavity for SHG enhancement. The monolayer WS_2 is laid on top of the SiO_2/Si substrate with holes (left panel). The right panel shows optical images of SH signals on cavity (up) and off cavity (bottom) under the same pump power.[126] (d) Illustration of SHG and SFG from the GaSe-silicon hybrid metasurface. Inset: schematic of L-shaped silicon meta-atom.[147] (e) Schematic of monolayer WS_2-dielectric PC waveguide hybrid metasurface for efficient frequency mixing process.[123] (f) Schematic illustration of monolayer MoS_2–TiO_2 nanorods-DBR hybrid metasurface for various temporal pulse-shaping operations (left panel). The side view of the meta-atom is composed of in-plane symmetry broken TiO_2 nanorods and TiO_2–SiO_2 DBR (right panel).[150]

Moreover, hybrid nonlinear metasurfaces can also be flexibly constructed by combining a variety of materials other than 2D materials.[151–165] Figure 5(a) depicts a four-channel multiplexed third-harmonic holographic imaging technique using a chiral Au–ZnO hybrid metasurface.[151] Specifically, the S-shaped gold nanoholes serve as phase modulation plates, while the ZnO is filled in S-shaped Au nanoholes, functioning as a THG source. Under the excitation of LCP or RCP fundamental wave, the LCP and RCP components of the TH hologram can be designed independently. This work has demonstrated circular dichroism of approximately 0.38 and a significant TH conversion efficiency of up to 10^{-5}, which will contribute to the new generation of optical encryption and optical signal processing.

Another dielectric material, $LiNbO_3$, has attracted considerable interest for frequency conversion due to its large second-order nonlinear susceptibility and wide transparency range from ultraviolet to mid-infrared spectrum.[160] Researchers have proposed a SiO_2 photonic crystal that based on $LiNbO_3$ thin film substrate to construct the BIC light field,[152] as shown in Fig. 5(b). The incident light field can be efficiently localized in the $LiNbO_3$ thin film, and a resonant mode with a Q-factor of 980 supported by the metasurface leads to a tremendous enhancement of SHG, which is more than 1500 times stronger than that of bare $LiNbO_3$ thin film. Similarly, the quasi-BIC-$LiNbO_3$ hybrid metasurface can be utilized for broadband THz wave generation and enhancement.[166] Additionally, the nonlinear optical process can also be enhanced by the resonance with high Q-factor caused by symmetry breaking. Figure 5(c) shows a hybrid metasurface composed of III–V semiconductors like $Al_{0.85}Ga_{0.15}As$ and GaAs, which feature a configuration with broken symmetry.[153] Due to the strong field confinement within the Fano-resonant nanostructure, a multifold enhancement of SHG is achieved without considering the phase matching.

In addition, the well-known multi-quantum-well (MQW) metasurface is also a type of hybrid metasurface, which has been extensively studied.[45,52,154] Belkin *et al*. reported a relatively large second-order susceptibility ($\chi^{(2)} \sim 54$ nm/V) in the mid-infrared region (~ 8 μm) by coupling the plasmonic metasurface to an MQW semiconductor structure.[52] Subsequently, MQW-based hybrid metasurfaces were proven to be capable of producing circular dichroism and beam manipulation for SHG and THG,[154] as shown in Fig. 5(d).

In general, the hybrid nonlinear metasurfaces have substantially expanded the research of metasurface devices. They have promoted the development of nonlinear optical devices by implementing multi-dimensional light-field modulation, such as phase, polarization, and amplitude, which has provided a promising platform for developing high-efficiency and multifunctional nonlinear nanodevices.

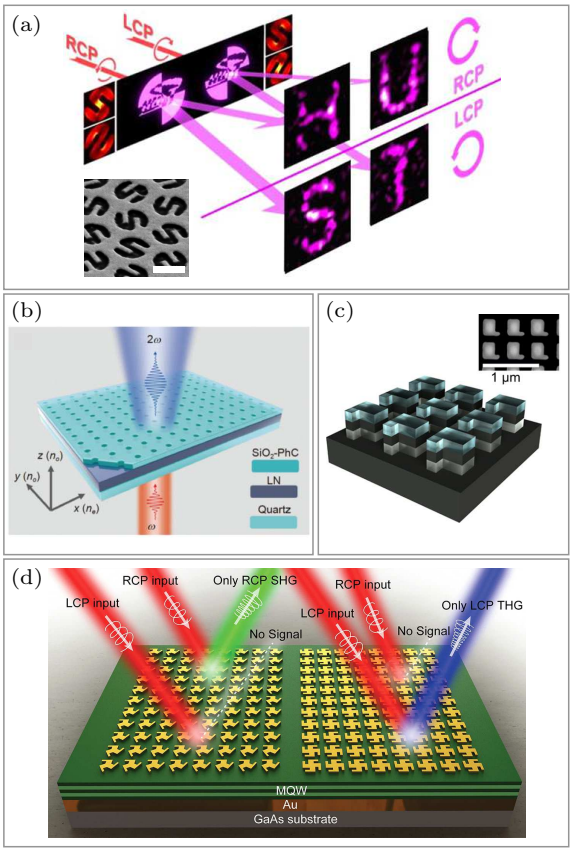

Fig. 5. (a) Schematic of ZnO–Au nanoholes hybrid metasurface for multiplexed TH holograms with four channels. Inset: SEM image of S-shaped nanoholes, the scale bar is 800 nm.[151] (b) Schematic of $LiNbO_3$–SiO_2 photonic crystal hybrid metasurface for SHG enhancement.[152] (c) Schematic of broken symmetry hybrid metasurface based on Fano resonance for SHG enhancement. Inset: SEM image of L-shaped meta-atoms.[153] (d) Schematic illustration of MQW-based hybrid metasurface composed of $C3$ and $C4$ rotational symmetry for chiral SHG and THG manipulation, respectively.[154]

3.3. Valleytronic modulation

The modulation of valley photons is a frontier research field, wherein the optical nanostructures provide an indelible contribution. TMDCs possess two degenerate yet unequivalent valleys (K' and K) located at the extreme points of the energy band within the Brillouin zone.[167] Owing to the natural inversion symmetry breaking, opposite Berry curvature is formed at the K' and K valleys, which corresponds to opposite orbital angular momentum respectively.[168,169] As a result of spin–orbit coupling, the spin states of electrons in monolayer TMDCs become mutually locked with their corresponding valleys, leading to a specific selectivity of electrons in different valleys to circularly polarized excitation, as illustrated in the inset of Fig. 6(a). The resulting valley degree of freedom is called valley pseudospin, which is a new degree of freedom in addition to the charge and spin, that has given rise to the emerging field of valleytronics.[170,171]

The emission of valley excitons carries valley information, enabling the transfer of information from electrons to photons and providing a new means of transmitting and storing information. Valleytronics has garnered widespread attention

in recent years due to its numerous advantages over conventional electronics, including higher processing speed, lower power consumption, greater integration, and reduced information loss.[171–178] Through the incorporation of electrodes to MoS_2, researchers are able to observe and control the valley Hall effect (VHE), opening up the possibilities for leveraging valley degrees of freedom as information carriers for next-generation electronics and optoelectronics.[169,179] However, practical applications of valleytronic devices still face certain limitations. Firstly, VHE typically requires low temperatures, which is unfavorable for the application of valleytronics at room temperature. Secondly, the lifetime of valley excitons in monolayer TMDCs is extremely short,[173,180,181] and there is competition between spontaneous radiative and non-radiative processes during the recombination of valley excitons, leading to low photoluminescence (PL) efficiency. Thirdly, phonon assisted intervalley scattering in monolayer TMDCs may lead to valley mixing, resulting in low valley polarization.[182–185] Finally, the photons emitted by valley excitons are usually scattered in all directions in free space, which poses a challenge for efficiently collecting valley emission.

To overcome the limitations in the development of valleytronics, researchers have conducted forward-looking works by combining TMDCs with nanostructures.[186–188] The propagation characteristics of the surface plasmon polaritons (SPP) can be utilized to separate valley excitons into different directions by introducing the photonic spin Hall effect (PSHE).[189–192] In 2018, Kuipers *et al*. coupled the valley pseudospin in WS_2 with the transverse optical spin angular momentum (t-OSAM) induced by SPP in Ag nanowires, achieving the separation of valley excitons at room temperature.[193] As shown in Fig. 6(a), the valley pseudospin of WS_2 can be coupled with t-OSAM of the same handedness, and photons from different valleys will propagate in the opposite directions along the Ag nanowire. Subsequently, they utilize the local t-OSAM in ZnO nanowires to selectively excite valley pseudospin in few-layer WS_2, resulting in the reversal of the propagation direction of valley photons in the waveguide.[194] Likewise, by coupling monolayer TMDCs to asymmetric nanogrooves, the asymmetric SPP modes can also be induced in groove waveguides through PSHE caused by spatial asymmetry.[195] Figure 6(b) presents a novel approach for separation and preservation of valley photons.[196] In this scheme, a monolayer WS_2 is sandwiched between an Au film and TiO_2 nanowires. The valley pseudospin of WS_2 is intelligently encoded and stored in the beating patterns generated by the interference of gap modes supported in the waveguide gap. High-fidelity propagation and directional routing of WS_2 valley photons are realized for the first time at room temperature, as shown in Fig. 6(b). This hybrid system not only showcases the valley fidelity of up to 98%, but also makes subsequent use of the separated valley information, such as nonreciprocal valley photon circulator and binary encoding.

In addition to valley excitons separation, hybrid metasurfaces have also been utilized to detect and enhance valley dark excitons that are difficult to collect due to the near-field radiation attenuation or out of plane dipole radiation of excitons,[197,198] which has prominent value for the modulation of photon information. Similarly, the hybrid structures also offer an efficient route for probing valley coherence.[199] As shown in Fig. 6(c), the polarization-dependent metasurface is coupled with a monolayer MoS_2, which generates an anisotropic vacuum field in close proximity to the monolayer MoS_2. This work theoretically demonstrates the spontaneous generation of valley coherence.

Besides the near-field enhancement, hybrid metasurfaces also exhibit remarkable functionality in manipulating valley photons. In 2019, Hu *et al*. proposed a novel nonlinear optical interface for efficient coherent steering of nonlinear valley photons in monolayer WS_2.[200] As shown in Fig. 6(d), a hybrid metasurface is formed by a plasmonic metasurface and monolayer WS_2. By introducing the P–B phase into the gold nanoholes, the SH valley photons from the K and K' valleys of WS_2 can be controlled and directed. This hybrid metasurface system can also be employed to manipulate the radiation direction of valley excitons.[201] As shown in Fig. 6(e), the plasmonic metasurface can induce an additional momentum that is related to the array period on the geometric phase gradient, resulting in the propagation direction of the SPP mode being locked by the optical spin–orbit interaction. Consequently, excitons with distinct valley polarizations manifest chirality-dependent propagation on the metasurface, as shown in Fig. 6(e). The platform presented in this study achieves a high valley contrast of up to 40% and stabilizes the intervalley coherence at 5%–8%.

In addition, the near-field local coupling induced by hybrid systems based on localized surface plasmons (LSP) can achieve effective enhancement of valley-polarized PL at the nanoscale.[202,203] Figure 6(f) presents an Au–MoS_2 hybrid metasurface, where the near-field coupling enables effective energy transfer from the Au metasurface to the monolayer MoS_2, leading to the enhancement of PL by over 10 times.[203] The chiral near-field induced by LSP in hybrid metasurfaces can also modulate the valley-polarized PL.[187,204–206] As shown in Fig. 6(g), a hybrid metasurface for the modulation of MoS_2 valley-polarized PL has been reported.[204] The MoS_2 monolayer is sandwiched between gold film and chiral Au metasurface, and the generation and radiation of valley excitons can be modulated by near-field interaction, thereby modulating the valley polarization. Similar principles are used to modulate the circular dichroism of WSe_2 PL radiation at low temperatures.[205] In addition, a designed LSP

resonant hybrid system can also tune the emission direction of the valley photons.[207,208] Lu *et al*. have fabricated a three-dimensional V-shaped antenna with chiral characteristics,[208] the antenna includes two gold nanorods with monolayer MoS_2 sandwiched in between them, as shown in Fig. 6(h). The interaction between light and matter can be significantly enhanced by forming LSP resonance in the overlapping region of nanorods, leading to an enhancement of PL by about three orders of magnitude. Furthermore, the far-field radiation direction of monolayer MoS_2 can be modulated from isotropic to unidirectional through the near-field coupling and far-field interference of nanoantennas. The chiral coupling characteristics in the hybrid system increase the valley polarization of TMDCs from 18% to 47%.

The aforementioned studies collectively indicate the outstanding performance of hybrid systems in valleytronics. The hybrid systems offer a concise and reliable approach for leveraging the valley degrees of freedom, and advance the research on nonlinear, quantum, and valleytronic nanodevices at room temperature.

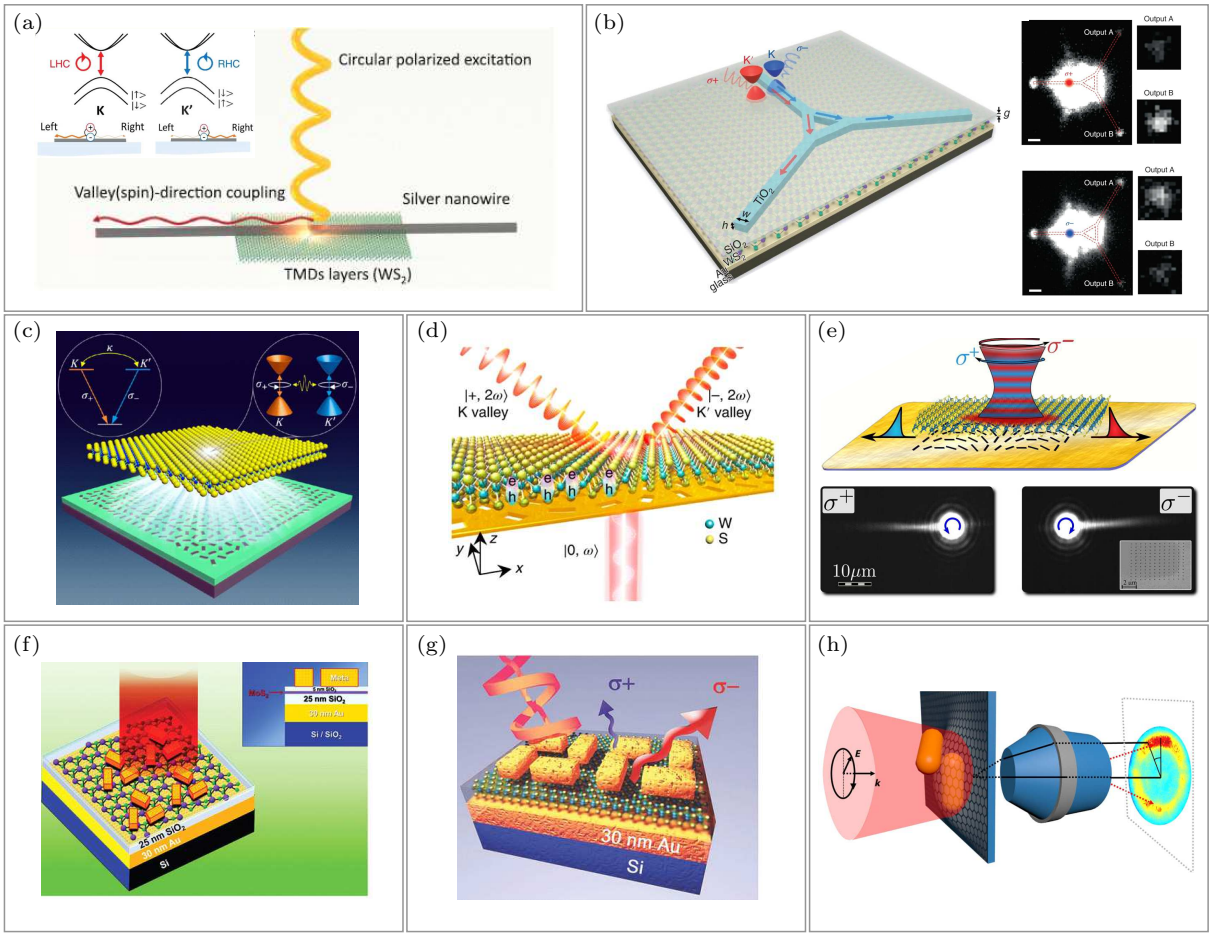

Fig. 6. (a) Schematic illustration of WS_2–Ag nanowire hybrid system for directional emission of valley excitons in WS_2. Inset: Schematic diagram of optical selection rules and directional coupling of WS_2 valley exciton.[193] (b) Schematic illustration of Au–WS_2–SiO_2–TiO_2 hybrid system for directional routing of WS_2 valley photons (left panel). The right panel shows the experimental results of the valley router under $\sigma+$ (up) and $\sigma-$ (bottom) excitations, the scale bar is 1 μm.[196] (c) Schematic of a hybrid metasurface composed of designed polarization-dependent metasurface and suspended monolayer TMDCs for spontaneous generation of valley coherence.[199] (d) Schematic illustration of Au–WS_2 hybrid metasurface for coherent steering of SH valley photons. The $|0,\omega\rangle$ denotes a linearly polarized fundamental wave, and the $|+,2\omega\rangle$ and $|-,2\omega\rangle$ denote RCP and LCP second-harmonic beams, respectively.[200] (e) Schematic of a hybrid metasurface composed of WS_2 and plasmonic array for manipulation of valley directional emission (upper panel). The lower panel shows the experimental real-space leakage radiation image of the SPP launched by $\sigma+$ (left) and $\sigma-$ (right) excitations on the plasmonic metasurface, the inset shows the SEM image of the hybrid metasurface.[201] (f) Schematic of a MoS_2–Au nanorods hybrid metasurface for near-field coupling and energy transfer. The MoS_2 monolayer is sandwiched between Au nanorods and Au film. Inset: side view of the hybrid system.[203] (g) Schematic of a MoS_2–Au nanorods hybrid metasurface for modulation of valley polarization. The MoS_2 monolayer is sandwiched between chiral Au nanorods and Au film.[204] (h) Schematic of directional emission measurements of MoS_2–Au nanorods hybrid system.[208]

3.4. Quantum technologies

Recently, the application of metasurfaces in quantum optics has garnered increasing interest. The interaction between light and matter will give rise to quantum behaviors under appropriate conditions, such as quantum entanglement,[209] quantum tunneling,[210] and quantum self-interference.[211] As mentioned previously, hybrid metasurfaces have demonstrated excellent capabilities for light-field modulation in classical optics. If extended to the field of quantum optics, hybrid metasurfaces hold the potential to tackle challenging

problems such as developing high-efficiency single-photon sources[212–214] and entangled photon sources,[42,215–220] as well as enabling efficient modulation and detection of quantum processes.[221–227]

Metasurfaces are considered an indispensable technique for enhancing quantum emission.[228,229] The traditional single-photon source relies on the spontaneous emission of a two-level system.[230] The rate of single-photon spontaneous emission can be increased by combining metasurfaces with quantum dots (QDs).[212] As shown in Fig. 7(a), the PL response of sparsely distributed QDs embedded in semiconductors can be significantly enhanced by coupling with plasmonic metasurfaces. The plasmonic metasurfaces improve the transfer of hot electrons and lead to a superlinear relationship between the PL response and the pump intensity even under weak excitation. This discovery is of great significance for designing efficient single-photon sources. Besides, the hybrid metasurfaces composed of metal and 2D materials can also enhance the emission efficiency of single-photon sources, which is more commonly employed compared to QDs. As shown in Fig. 7(b), a hybrid metasurface is developed by integrating plasmonic nanoparticles with 2D hexagonal boron nitride (hBN).[213] In this work, the coupling of hBN and nanoparticles array provides a high-quality and low-loss cavity, and the hybrid metasurface demonstrates a boost in emission efficiency and a decrease in PL lifetimes due to the amplified Purcell effect in the weak coupling region, while preserving the single-photon characteristics of the emitter.

The generation of entangled photon pairs is a crucial component of quantum communication technologies. Currently, one of the most widely used technologies for generating entangled photon pairs is spontaneous parametric down conversion (SPDC).[231] However, the efficiency of SPDC is exceedingly low in the usual spontaneous quantum nonlinear processes owing to its very weak nature. Numerous methods have been implemented to enhance the efficiency of SPDC, including resonators,[232] waveguides,[233] and photonic crystals.[234] But it is still challenging to integrate due to their cumbersome size. The proposal of metasurfaces effectively resolves this aporia and enables the generation of entangled photon pairs utilizing SPDC within the visible and near-infrared spectral range. Tsai *et al.*[215] integrated metalens with a BBO crystal to focus the laser at the center of the BBO crystal, as shown in Fig. 7(c). They successfully achieved path entanglement of high-dimensional photon pairs and generated entangled photon pairs of up to six photons, as well as effortlessly switching between high-dimensional entangled states. This work provides a unique platform for integrated devices of quantum light sources. In 2019, Neshev *et al.*[216] proposed an optical nanoantennas configuration that exhibits Mie-resonance at both pump and two-photon wavelengths, as shown in Fig. 7(d), with a photon-pair production rate through SPDC of 35 Hz. This work is the first proposed spontaneous entangled photon-pair generation source at the nanoscale, opening up a pathway for designing individual nanoantenna to resonantly enhance the SPDC process. Additionally, in the same year, Okoth *et al.*[235] reported the first-ever observation of SPDC without phase matching. A $LiNbO_3$ crystal, with a thickness of 6 μm, was employed as a planar geometry source. The momentum conservation requirement was relaxed by capitalizing on the uncertainty relation of the position–momentum of the thin layer. In 2021, Jin *et al.*[217] proposed a hybrid metasurface that consisted of periodic silver nanostripes and bulk $LiNbO_3$, as shown in Fig. 7(e). This hybrid metasurface accomplished the efficient production of entangled photon pairs through SPDC at room temperature, with highly coherent emission directions perpendicular to the metasurface.

In addition to plasmonic nanostructures, SPDC can also be achieved in hybrid dielectric nonlocal metasurfaces.[218] As depicted in Fig. 7(f), an extra enhancement of the SPDC process in $LiNbO_3$ thin film can be achieved through the guided mode resonance of SiO_2 gratings, which leads to a 450-fold increase in the production rate of entangled photon pairs compared to bare $LiNbO_3$ thin film. Moreover, the concept of BIC can be introduced to dielectric metasurfaces. Kivshar *et al.*[236] put forth a new strategy that remarkably enhances nonlinear response at the micro-nano scale by adopting the concept of BIC. The $\chi^{(2)}$ in AlGaAs nanoantennas is comparable to the cutting-edge on-chip scale whispering gallery mode resonators.[237] Furthermore, similar methods can be adapted to non-classical fields.[238] Chekhova *et al.*[219] prepared an array structure of GaAs by introducing symmetric protected quasi-BIC resonance, as shown in Fig. 7(g). The efficiency of photon-pair emission was at least three orders of magnitude higher than that of bare GaAs thin film.

The flexible capability of metasurfaces to modulate the electromagnetic field enables substantial degrees of freedom in photon emission. Recent studies have shown that metasurfaces can achieve complex control over quantum light sources, including phase modulation[214,221,224] and manipulation of emission direction.[223] Figure 7(h) shows a novel approach to generating single-photon carrying spin angular momentum (SAM) at room-temperature.[225] The hybrid metasurface consisting of a stand-alone quantum emitter and concentric periodic width-varying dielectric nanoridges produces highly directional circularly polarized light, wherein the optical metasurface facilitates the transformation of nonradiative coupling between quantum emitters and surface plasmons into a collimated stream of SAM encoded single-photon with designed handedness. In addition, researchers have reported the realization of chiral single-photon emission through the cou-

pling of strain-induced quantum emitters in monolayer WSe_2 with the whispering gallery mode of a Si_3N_4 ring-shaped resonators,[226] as shown in Fig. 7(i). In this hybrid system, the intrinsic spin states of the quantum emitter are coupled to the propagation direction of the cavity mode, resulting in the spin–orbit locking, which leads to the chiral single-photon emission.

To summarize, hybrid metasurfaces have shown promising potential in the field of quantum optics. The integration of metasurfaces and nonlinear materials has greatly improved the efficiency of generating single-photon and entangled photon pairs, and provided more degrees of freedom for modulating quantum states, enabling a range of functions that cannot be achieved in the classical optics.

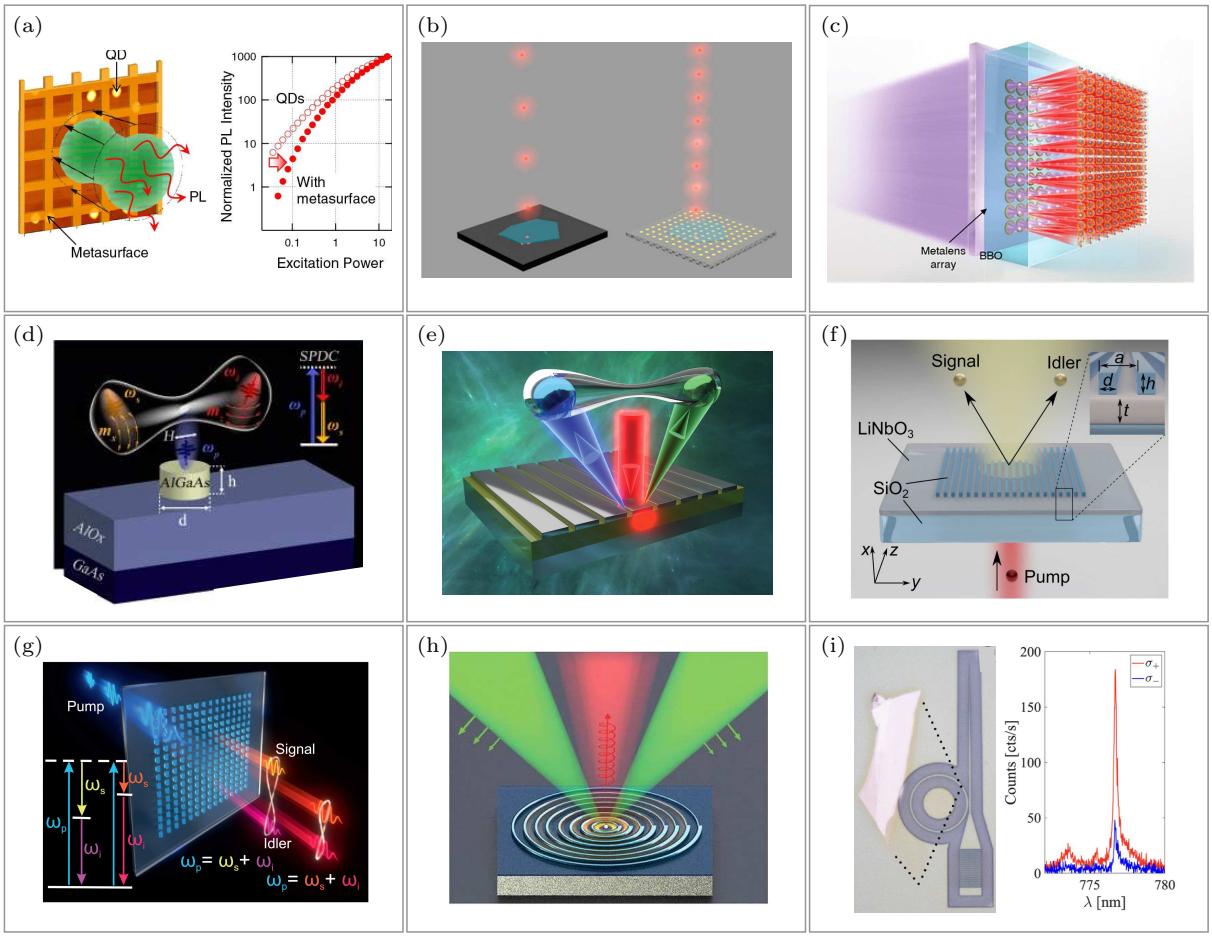

Fig. 7. (a) Schematic illustration of a quantum dots-metasurface hybrid system for improving the single-photon emission (left panel). Superlinear PL responses of quantum dots with (solid circle) and without (hollow circle) metasurface (right panel).[212] (b) Schematic of hBN-plasmonic particles array hybrid metasurface for enhancing the quantum emission.[213] (c) Schematic of BBO-metalens hybrid system for quantum source.[215] (d) Schematic of entangled photon-pair emission of AlGaAs nanoantenna based on SPDC.[216] (e) Schematic of entangled photon-pair generation through SPDC in hybrid metasurfaces composed of Ag nanostripes and $LiNbO_3$.[217] (f) Schematic of hybrid metasurface composed of SiO_2 gratings and $LiNbO_3$ thin film for efficient generation of spatially entangled photon pairs.[218] (g) Schematic of SPDC using symmetry-protected quasi-BIC resonances in a dielectric metasurface.[219] (h) Schematic of hybrid metasurface for the generation of circularly polarized single-photon. A nanodiamond containing a nitrogen vacancy center is located in the center of a metasurface composed of hydrogen silsesquioxane circular nanoridges with azimuthally varying widths deterministically fabricated atop SiO_2 spacer and Ag substrate.[225] (i) Optical image of hybrid metasurface device for single-photon emission, the monolayer WSe_2 is outlined by the dotted black lines (left panel). PL spectrum of chiral emission (right panel).[226]

4. Conclusions and perspectives

We present a thorough review of the recent advances in hybrid nonlinear metasurfaces. Our focus centers on the innovation of hybrid nonlinear metasurfaces in light-field modulation, viewed from the vantage point of conventional plasmonic and all-dielectric nonlinear metasurfaces. We discuss the pivotal role of hybrid systems in four essential aspects: multifunctional phase modulation, nonlinearity enhancement, valleytronic modulation, and quantum technologies. The hybrid metasurfaces are in the joint fields of stable wavefront manipulation, nonlinear metasurfaces and frequency conversions, providing a potential platform for nonlinear light-field modulation. Particularly, the hybrid systems comprising nanostructures and 2D materials have shown remarkable capabilities in modulating valley photons and entangled photons, while also have advantageous for integration. This provides a great impetus for the fields of valleytronics and quantum optics. It follows that the combination of nanostructures and nonlinear

materials turns out to have synergistic benefits, and their rich photophysical properties make various novel concepts of photonic devices possible. Nonetheless, challenges still remain.

(i) The fabrication of hybrid structures usually involves combining multiple nanomanufacturing processes, given that these structures typically comprise various materials. For the nanostructures that required high precision, the current fabrication methods like electron beam lithography and photolithography cannot guarantee the yield. Therefore, higher requirements are placed on nanofabrication techniques.[239]

(ii) The ultra-thin size of hybrid metasurfaces results in a relatively short effective length of light–matter interaction, mostly at the subwavelength scale. Therefore, their nonlinear conversion efficiency is still lower compared to conventional nonlinear crystals like BBO, LBO, etc. This greatly restricts the application of metasurfaces in integrated devices. Hence, it is necessary to explore new systems with higher nonlinear responses to further enhance the nonlinear conversion efficiency. A feasible approach is to initiate with the resonant modes of nanostructures and apply the mode coupling theory to explore novel electromagnetic resonance modes. For instance, introduce the concept of BIC or other resonant modes and construct optical cavities with higher Q-factor to generate higher-order nonlinear signals.[93,240,241] Another viable approach is to initiate with nonlinear materials, such as the multi-layer stacking of 2D materials that exhibits superlinear second-order nonlinearity,[242–245] which provides a powerful means for enhancing processes like SPDC and optical parametric amplification (OPA).[246,247] Additionally, attempts can be made to modify the atomic concentration in the 2D material heterostructures, such as chemical doping, to modulate their overall nonlinear properties.[248]

(iii) Enhancing the nonlinear conversion efficiency would facilitate the extension of light-field modulation to higher-order nonlinear effects, thereby enabling the achievement of more functions. The research on light-field modulation in hybrid systems based on dielectric-2D materials is still in its infancy. Dielectric metasurfaces, with their ability to attain ultra-high Q-factors and damage thresholds, hold promise for higher-order harmonic light-field modulation.

(iv) Research on hybrid metasurfaces in quantum optics is ongoing, we believe that the full potential of metasurfaces has yet to be fully exploited. Building upon the enhanced SPDC process facilitated by hybrid metasurfaces, the incorporation of phase modulation is expected to enable the realization of a more stable and multi-dimensionally tunable integrated multiphoton-entangled source. And the tunable phase-change materials can be introduced and expected to modulate the photon emission direction and polarization on quantum coupled metasurfaces, through temperature and voltage control. Therefore, the potential for further development of quantum hybrid metasurfaces is immense.

(v) Valleytronic devices are still far from practical applications due to the limitations such as low valley polarization, low radiation efficiency of valley excitons, and short propagation distance of valley photons. Based on the multidimensional modulation of hybrid systems on valley polarization, new hybrid spin-valley-photon ecosystems at the nanoscale can be further explored to improve the coupling efficiency between valley photons and nanostructures and overcome the aforementioned limitations. This is of paramount significance for constructing large-scale valleytronic network systems at room temperature, and has broad prospects in valley-photon computing chips in the future.

In summary, the hybrid nonlinear metasurfaces in light-field modulation are currently undergoing in-depth research and rapid development. With the exploration of advanced nanofabrication techniques, emerging materials, and new physics, the aforementioned challenges may be resolved. We expect that the future research on hybrid metasurfaces will yield more photonics devices with brand-new functions, and further broaden the horizons of nanophotonics.

Acknowledgments

Project supported by the National Natural Science Foundation of China (Grant Nos. 12274157, 12274334, 91850113, 12021004, and 11904271), the Natural Science Foundation of Hubei Province of China (Grant No. 2023AFA076), and the Basic and Applied Basic Research Major Program of Guangdong Province of China (Grant No. 2019B030302003).

References

[1] Soukoulis C M and Wegener M 2011 *Nat. Photonics* **5** 523
[2] Hess O, Pendry J B, Maier S A, Oulton R F, Hamm J M and Tsakmakidis K L 2012 *Nat. Mater.* **11** 573
[3] Zheludev N I and Kivshar Y S 2012 *Nat. Mater.* **11** 917
[4] Chen H T, Taylor A J and Yu N 2016 *Rep. Prog. Phys.* **79** 076401
[5] Yu N, Genevet P, Kats M A, Aieta F, Tetienne J P, Capasso F and Gaburro Z 2011 *Science* **334** 333
[6] Ni X, Emani N K, Kildishev A V, Boltasseva A and Shalaev V M 2012 *Science* **335** 427
[7] Sun S, He Q, Xiao S, Xu Q, Li X and Zhou L 2012 *Nat. Mater.* **11** 426
[8] Kildishev A V, Boltasseva A and Shalaev V M 2013 *Science* **339** 1232009
[9] Meinzer N, Barnes W L and Hooper I R 2014 *Nat. Photonics* **8** 889
[10] Yu N and Capasso F 2014 *Nat. Mater.* **13** 139
[11] Anandan J 1992 *Nature* **360** 307
[12] Berry M V 1984 *Proc. Math. Phys. Eng. Sci.* **392** 45
[13] Chen X, Huang L, Muhlenbernd H, Li G, Bai B, Tan Q, Jin G, Qiu C W, Zhang S and Zentgraf T 2012 *Nat. Commun.* **3** 1198
[14] Jiang S C, Xiong X, Hu Y S, Jiang S W, Hu Y H, Xu D H, Peng R W and Wang M 2015 *Phys. Rev. B* **91** 125421
[15] Kang M, Feng T, Wang H T and Li J 2012 *Opt. Express* **20** 15882
[16] Huang L, Chen X, Muhlenbernd H, Li G, Bai B, Tan Q, Jin G, Zentgraf T and Zhang S 2012 *Nano Lett.* **12** 5750
[17] Yu N, Genevet P, Aieta F, Kats M A, Blanchard R, Aoust G, Tetienne J P, Gaburro Z and Capasso F 2013 *IEEE J. Sel. Top. Quantum Electron.* **19** 4700423

[18] Chong K E, Staude I, James A, Dominguez J, Liu S, Campione S, Subramania G S, Luk T S, Decker M, Neshev D N, Brener I and Kivshar Y S 2015 *Nano Lett.* **15** 5369

[19] Yu N, Aieta F, Genevet P, Kats M A, Gaburro Z and Capasso F 2012 *Nano Lett.* **12** 6328

[20] Li Q T, Dong F, Wang B, Gan F, Chen J, Song Z, Xu L, Chu W, Xiao Y F, Gong Q and Li Y 2016 *Opt. Express* **24** 16309

[21] Kamali S M, Arbabi E, Arbabi A and Faraon A 2018 *Nanophotonics* **7** 1041

[22] Qiu C W, Zhang T, Hu G and Kivshar Y 2021 *Nano Lett.* **21** 5641

[23] Dai Z, Hu G, Ou Q, Zhang L, Xia F, Garcia-Vidal F J, Qiu C W and Bao Q 2020 *Chem. Rev.* **120** 6197

[24] Lin D, Fan P, Hasman E and Brongersma M L 2014 *Science* **345** 298

[25] Aieta F, Kats M A, Genevet P and Capasso F 2015 *Science* **347** 1342

[26] Khorasaninejad M, Chen W T, Devlin R C, Oh J, Zhu A Y and Capasso F 2016 *Science* **352** 1190

[27] Wang Q, Rogers E T F, Gholipour B, Wang C M, Yuan G, Teng J and Zheludev N I 2015 *Nat. Photonics* **10** 60

[28] Chen W T, Yang K Y, Wang C M, Huang Y W, Sun G, Chiang I D, Liao C Y, Hsu W L, Lin H T, Sun S, Zhou L, Liu A Q and Tsai D P 2014 *Nano Lett.* **14** 225

[29] Ni X, Kildishev A V and Shalaev V M 2013 *Nat. Commun.* **4** 2807

[30] Huang L, Chen X, Mühlenbernd H, Zhang H, Chen S, Bai B, Tan Q, Jin G, Cheah K W, Qiu C W, Li J, Zentgraf T and Zhang S 2013 *Nat. Commun.* **4** 2808

[31] Huang Y W, Chen W T, Tsai W Y, Wu P C, Wang C M, Sun G and Tsai D P 2015 *Nano Lett.* **15** 3122

[32] Zheng G, Muhlenbernd H, Kenney M, Li G, Zentgraf T and Zhang S 2015 *Nat. Nanotechnol.* **10** 308

[33] Huang L, Muhlenbernd H, Li X, Song X, Bai B, Wang Y and Zentgraf T 2015 *Adv. Mater.* **27** 6444

[34] Wen D, Yue F, Li G, Zheng G, Chan K, Chen S, Chen M, Li K F, Wong P W, Cheah K W, Pun E Y, Zhang S and Chen X 2015 *Nat. Commun.* **6** 8241

[35] Wu P C, Tsai W Y, Chen W T, Huang Y W, Chen T Y, Chen J W, Liao C Y, Chu C H, Sun G and Tsai D P 2017 *Nano Lett.* **17** 445

[36] Chen S, Cai Y, Li G, Zhang S and Cheah K W 2016 *Laser Photonics Rev.* **10** 322

[37] Devlin R C, Ambrosio A, Rubin N A, Mueller J P B and Capasso F 2017 *Science* **358** 896

[38] Maguid E, Yulevich I, Veksler D, Kleiner V, Brongersma M L and Hasman E 2016 *Science* **352** 1202

[39] Li G, Kang M, Chen S, Zhang S, Pun E Y, Cheah K W and Li J 2013 *Nano Lett.* **13** 4148

[40] Boyd R W 2008 *Nonlinear Optics* (3rd edn.) (America: Academic Press)

[41] Keller U 2003 *Nature* **424** 831

[42] Santiago-Cruz T, Fedotova A, Sultanov V, Weissflog M A, Arslan D, Younesi M, Pertsch T, Staude I, Setzpfandt F and Chekhova M 2021 *Nano Lett.* **21** 4423

[43] Li W, Chen B, Meng C, Fang W, Xiao Y, Li X, Hu Z, Xu Y, Tong L, Wang H, Liu W, Bao J and Shen Y R 2014 *Nano Lett.* **14** 955

[44] Nabet B 2016 *Photodetectors: Materials, Devices and Applications* (1st edn.) (London: Woodhead Publishing)

[45] Tymchenko M, Gomez-Diaz J S, Lee J, Nookala N, Belkin M A and Alu A 2015 *Phys. Rev. Lett.* **115** 207403

[46] Li G, Chen S, Pholchai N, Reineke B, Wong P W, Pun E Y, Cheah K W, Zentgraf T and Zhang S 2015 *Nat. Mater.* **14** 607

[47] Li G, Zhang S and Zentgraf T 2017 *Nat. Rev. Mater.* **2** 17010

[48] Overvig A C, Malek S C and Yu N 2020 *Phys. Rev. Lett.* **125** 017402

[49] Lu J, Liu X, Bruch A W, Zhang L, Wang J, Yan J and Tang H X 2020 *Opt. Lett.* **45** 4499

[50] Lu J, Surya J B, Liu X, Xu Y and Tang H X 2019 *Opt. Lett.* **44** 1492

[51] O'Brien K, Suchowski H, Rho J, Salandrino A, Kante B, Yin X and Zhang X 2015 *Nat. Mater.* **14** 379

[52] Nookala N, Lee J, Tymchenko M, Sebastian G D J, Demmerle F, Boehm G, Lai K, Shvets G, Amann M C, Alu A and Belkin M 2016 *Optica* **3** 283

[53] Minerbi E, Keren-Zur S and Ellenbogen T 2019 *Nano Lett.* **19** 6072

[54] Linden S, Niesler F B, Forstner J, Grynko Y, Meier T and Wegener M 2012 *Phys. Rev. Lett.* **109** 015502

[55] Segal N, Keren-Zur S, Hendler N and Ellenbogen T 2015 *Nat. Photonics* **9** 180

[56] Keren-Zur S, Avayu O, Michaeli L and Ellenbogen T 2015 *ACS Photonics* **3** 117

[57] Kruk S S, Decker M, Staude I, Schlecht S, Greppmair M, Neshev D N and Kivshar Y S 2014 *ACS Photonics* **1** 1218

[58] Yang X, Zhang C, Wan M, Chen Z and Wang Z 2016 *Opt. Lett.* **41** 2938

[59] Ye W, Zeuner F, Li X, Reineke B, He S, Qiu C W, Liu J, Wang Y, Zhang S and Zentgraf T 2016 *Nat. Commun.* **7** 11930

[60] Chen Y, Yang X and Gao J 2018 *Adv. Opt. Mater.* **6** 1800646

[61] Chen S, Reineke B, Li G, Zentgraf T and Zhang S 2019 *Nano Lett.* **19** 6278

[62] Veysi M, Guclu C, Boyraz O and Capolino F 2017 *J. Opt. Soc. Am. B* **34** 374

[63] Li G, Wu L, Li K F, Chen S, Schlickriede C, Xu Z, Huang S, Li W, Liu Y, Pun E Y B, Zentgraf T, Cheah K W, Luo Y and Zhang S 2017 *Nano Lett.* **17** 7974

[64] Schlickriede C, Waterman N, Reineke B, Georgi P, Li G, Zhang S and Zentgraf T 2018 *Adv. Mater.* **30** 1703843

[65] Walter F, Li G, Meier C, Zhang S and Zentgraf T 2017 *Nano Lett.* **17** 3171

[66] Tang Y, Intaravanne Y, Deng J, Li K F, Chen X and Li G 2019 *Phys. Rev. Appl.* **12** 024028

[67] Mao N, Deng J, Zhang X, Tang Y, Jin M, Li Y, Liu X, Li K, Cao T, Cheah K, Wang H, Ng J and Li G 2020 *Nano Lett.* **20** 7463

[68] Chen S, Zeuner F, Weismann M, Reineke B, Li G, Valev V K, Cheah K W, Panoiu N C, Zentgraf T and Zhang S 2016 *Adv. Mater.* **28** 2992

[69] Mao N, Zhang G, Tang Y, Li Y, Hu Z, Zhang X, Li K, Cheah K and Li G 2022 *Proc. Natl. Acad. Sci. USA* **119** e2204418119

[70] Niu J, Zhai Y, Han Q, Liu J and Yang B 2021 *Opt. Lett.* **46** 162

[71] Wang L, Kruk S, Koshelev K, Kravchenko I, Luther-Davies B and Kivshar Y 2018 *Nano Lett.* **18** 3978

[72] Gao Y, Fan Y, Wang Y, Yang W, Song Q and Xiao S 2018 *Nano Lett.* **18** 8054

[73] Bar-David J and Levy U 2019 *Nano Lett.* **19** 1044

[74] Grinblat G 2021 *ACS Photonics* **8** 3406

[75] Liu S, Vabishchevich P P, Vaskin A, Reno J L, Keeler G A, Sinclair M B, Staude I and Brener I 2018 *Nat. Commun.* **9** 2507

[76] Xu L, Saerens G, Timofeeva M, Smirnova D A, Volkovskaya I, Lysevych M, Camacho-Morales R, Cai M, Zangeneh K K, Huang L, Karouta F, Tan H H, Jagadish C, Miroshnichenko A E, Grange R, Neshev D N and Rahmani M 2020 *ACS Nano* **14** 1379

[77] Schlickriede C, Kruk S S, Wang L, Sain B, Kivshar Y and Zentgraf T 2020 *Nano Lett.* **20** 4370

[78] Liu B, Sain B, Reineke B, Zhao R, Meier C, Huang L, Jiang Y and Zentgraf T 2020 *Adv. Opt. Mater.* **8** 1902050

[79] Gigli C, Marino G, Artioli A, Rocco D, De Angelis C, Claudon J, Gérard J M and Leo G 2021 *Optica* **8** 269

[80] Hahnel D, Golla C, Albert M, Zentgraf T, Myroshnychenko V, Forstner J and Meier C 2023 *Light Sci. Appl.* **12** 97

[81] Melik-Gaykazyan E V, Kruk S S, Camacho-Morales R, Xu L, Rahmani M, Zangeneh K K, Lamprianidis A, Miroshnichenko A E, Fedyanin A A, Neshev D N and Kivshar Y S 2017 *ACS Photonics* **5** 728

[82] Xu L, Rahmani M, Zangeneh K K, Lamprianidis A, Ghirardini L, Sautter J, Camacho-Morales R, Chen H, Parry M, Staude I, Zhang G, Neshev D and Miroshnichenko A E 2018 *Light Sci. Appl.* **7** 44

[83] Savinov V, Papasimakis N, Tsai D P and Zheludev N I 2019 *Commun. Phys.* **2** 69

[84] Cui X, Lai Y, Ai R, Wang H, Shao L, Chen H, Zhang W and Wang J 2020 *Adv. Opt. Mater.* **8** 2001173

[85] Koshelev K, Kruk S, Melik-Gaykazyan E, Choi J H, Bogdanov A, Park H G and Kivshar Y 2020 *Science* **367** 288

[86] Koshelev K, Bogdanov A and Kivshar Y 2019 *Sci. Bull.* **64** 836

[87] Gandolfi M, Tognazzi A, Rocco D, De Angelis C and Carletti L 2021 *Phys. Rev. A* **104** 023524

[88] Fang C, Yang Q, Yuan Q, Gu L, Gan X, Shao Y, Liu Y, Han G and Hao Y 2022 *Laser Photonics Rev.* **16** 2100498

[89] Koshelev K, Tang Y, Li K, Choi D Y, Li G and Kivshar Y 2019 *ACS Photonics* **6** 1639

[90] Xu L, Kamali K Z, Huang L, Rahmani M, Smirnov A, Camacho-Morales R, Ma Y, Zhang G, Woolley M, Neshev D and Miroshnichenko A E 2019 *Adv. Sci.* **6** 1802119

[91] Liu Z, Xu Y, Lin Y, Xiang J, Feng T, Cao Q, Li J, Lan S and Liu J 2019 *Phys. Rev. Lett.* **123** 253901

[92] Liu H, Guo C, Vampa G, Zhang J L, Sarmiento T, Xiao M, Bucksbaum P H, Vučković J, Fan S and Reis D A 2018 *Nat. Phys.* **14** 1006

[93] Zograf G, Koshelev K, Zalogina A, Korolev V, Hollinger R, Choi D Y, Zuerch M, Spielmann C, Luther-Davies B, Kartashov D, Makarov S V, Kruk S S and Kivshar Y 2022 *ACS Photonics* **9** 567

[94] Janisch C, Wang Y, Ma D, Mehta N, Elias A L, Perea-Lopez N, Terrones M, Crespi V and Liu Z 2014 *Sci. Rep.* **4** 5530

[95] Fan X, Jiang Y, Zhuang X, Liu H, Xu T, Zheng W, Fan P, Li H, Wu X, Zhu X, Zhang Q, Zhou H, Hu W, Wang X, Sun L, Duan X and Pan A 2017 *ACS Nano* **11** 4892

[96] Hsu C, Frisenda R, Schmidt R, Arora A, Vasconcellos S M, Bratschitsch R, Zant H S J and Castellanos-Gomez A 2019 *Adv. Opt. Mater.* **7** 1900239

[97] Kumar N, Najmaei S, Cui Q, Ceballos F, Ajayan P M, Lou J and Zhao H 2013 *Phys. Rev. B* **87** 161403

[98] Li Y, Rao Y, Mak K F, You Y, Wang S, Dean C R and Heinz T F 2013 *Nano Lett.* **13** 3329

[99] Woodward R I, Murray R T, Phelan C F, de Oliveira R E P, Runcorn T H, Kelleher E J R, Li S, Oliveira E C D, Fechine G J M, Eda G and Matos C J S 2016 *2D Mater.* **4** 011006

[100] Islam K M, Synowicki R, Ismael T, Oguntoye I, Grinalds N and Escarra M D 2021 *Adv. Photonics Res.* **2** 2000180

[101] Seyler K L, Schaibley J R, Gong P, Rivera P, Jones A M, Wu S, Yan J, Mandrus D G, Yao W and Xu X 2015 *Nat. Nanotechnol.* **10** 407

[102] Ribeiro-Soares J, Janisch C, Liu Z, Elías A L, Dresselhaus M S, Terrones M, Cançado L G and Jorio A 2015 *2D Mater.* **2** 045015

[103] Le C T, Clark D J, Ullah F, Senthilkumar V, Jang J I, Sim Y, Seong M J, Chung K H, Park H and Kim Y S 2016 *Ann. Phys.* **528** 551

[104] Wang G, Wong G K L and Ketterson J B 2001 *Appl. Opt.* **40** 5436

[105] Bond W L 1965 *J. Appl. Phys.* **36** 1674

[106] Shoji I, Kondo T, Kitamoto A, Shirane M and Ito R 1997 *J. Opt. Soc. Am. B* **14** 2268

[107] Papatryfonos K, Angelova T, Brimont A, Reid B, Guldin S, Smith P R, Tang M, Li K, Seeds A J, Liu H and Selviah D R 2021 *AIP Adv.* **11** 025327

[108] Zelmon D E and Small D L 1997 *J. Opt. Soc. Am. B* **14** 3319

[109] Autere A, Jussila H, Marini A, Saavedra J R M, Dai Y, Säynätjoki A, Karvonen L, Yang H, Amirsolaimani B, Norwood R A, Peyghambarian N, Lipsanen H, Kieu K, Abajo F J G and Sun Z 2018 *Phys. Rev. B* **98** 115426

[110] Wang R, Chien H C, Kumar J, Kumar N, Chiu H Y and Zhao H 2014 *ACS Appl. Mater. Interfaces* **6** 314

[111] Kumar N, Kumar J, Gerstenkorn C, Wang R, Chiu H Y, Smirl A L and Zhao H 2013 *Phys. Rev. B* **87** 121406

[112] Jiang T, Huang D, Cheng J, Fan X, Zhang Z, Shan Y, Yi Y, Dai Y, Shi L, Liu K, Zeng C, Zi J, Sipe J E, Shen Y R, Liu W T and Wu S 2018 *Nat. Photonics* **12** 430

[113] Nelson F J, Kamineni V K, Zhang T, Comfort E S, Lee J U and Diebold A C 2010 *Appl. Phys. Lett.* **97** 253110

[114] Zappettini A, D'Amore F, Pietralunga S M, Terio A, Martinelli M, Bliss D F and Callahan M J 2004 *Phys. Status Solidi (c)* **1** 997

[115] Hon N K, Soref R and Jalali B 2011 *J. Appl. Phys.* **110** 011301

[116] Green M A 2008 *Sol. Energy Mater. Sol. Cells* **92** 1305

[117] Li Y, Sun H, Gan L, Zhang J, Feng J, Zhang D and Ning C Z 2020 *Proc. IEEE* **108** 676

[118] Wen X, Gong Z and Li D 2019 *InfoMat* **1** 317

[119] Cong C, Shang J, Wang Y and Yu T 2018 *Adv. Opt. Mater.* **6** 1700767

[120] Autere A, Jussila H, Dai Y, Wang Y, Lipsanen H and Sun Z 2018 *Adv. Mater.* **30** 1705963

[121] Chen H, Corboliou V, Solntsev A S, Choi D Y, Vincenti M A, de Ceglia D, de Angelis C, Lu Y and Neshev D N 2017 *Light Sci. Appl.* **6** e17060

[122] Li D, Wei C, Song J, Huang X, Wang F, Liu K, Xiong W, Hong X, Cui B, Feng A, Jiang L and Lu Y 2019 *Nano Lett.* **19** 4195

[123] Guo Q, Ou Z, Tang J, Zhang J, Lu F, Wu K, Zhang D, Zhang S and Xu H 2020 *Nano Lett.* **20** 7956

[124] Zhang Z, Zhang L, Gogna R, Chen Z and Deng H 2020 *Solid State Commun.* **322** 114043

[125] Zhou Z K, Xu H F, Yu Y, Lin L and Wang X H 2021 *Laser Photonics Rev.* **15** 2100281

[126] Shi J, Wu X, Wu K, Zhang S, Sui X, Du W, Yue S, Liang Y, Jiang C, Wang Z, Wang W, Liu L, Wu B, Zhang Q, Huang Y, Qiu C W and Liu X 2022 *ACS Nano* **16** 13933

[127] Löchner F J F, George A, Koshelev K, Bucher T, Najafidehaghani E, Fedotova A, Choi D Y, Pertsch T, Staude I, Kivshar Y, Turchanin A and Setzpfandt F 2020 *ACS Photonics* **8** 218

[128] Xiao J, Ye Z, Wang Y, Zhu H, Wang Y and Zhang X 2015 *Light Sci. Appl.* **4** e366

[129] Zhao W, Wang K, Hong X, Wang B, Han X, Wang K, Liu W, Long H, Wang B and Lu P 2021 *Sci. Bull.* **66** 449

[130] Chen J, Wang K, Long H, Han X, Hu H, Liu W, Wang B and Lu P 2018 *Nano Lett.* **18** 1344

[131] Hong X, Hu G, Zhao W, Wang K, Sun S, Zhu R, Wu J, Liu W, Loh K P, Wee A T S, Wang B, Alu A, Qiu C W and Lu P 2020 *Research* **2020** 9085782

[132] Busschaert S, Flory N, Papadopoulos S, Parzefall M, Heeg S and Novotny L 2019 *Nano Lett.* **19** 6097

[133] Shi J, He X, Li Y, Zhang S and Xu H 2019 *ACS Photonics* **6** 3142

[134] Spreyer F, Zhao R, Huang L and Zentgraf T 2020 *Nanophotonics* **9** 351

[135] Guo W P, Liang W Y, Cheng C W, Wu W L, Wang Y T, Sun Q, Zu S, Misawa H, Cheng P J, Chang S W, Ahn H, Lin M T and Gwo S 2020 *Nano Lett.* **20** 2857

[136] Zhao W, Wang K, Hong X, Wang B, Han X, Long H, Wang B and Lu P 2020 *Nanoscale* **12** 13330

[137] Wang B, Wang K, Hong X, Sheng Y, Qian S and Lu P 2021 *Laser Photonics Rev.* **15** 2100031

[138] Chen H, Lu W B, Liu Z G and Geng M Y 2020 *ACS Photonics* **7** 1425

[139] Liu Z and Bai B 2017 *Opt. Express* **25** 8584

[140] Liu W, Hu B, Huang Z, Guan H, Li H, Wang X, Zhang Y, Yin H, Xiong X, Liu J and Wang Y 2018 *Photonics Res.* **6** 703

[141] Ma S, Wen S, Mi X and Zhao H 2023 *Opt. Commun.* **536** 129398

[142] Huang L, Krasnok A, Alu A, Yu Y, Neshev D and Miroshnichenko A E 2022 *Rep. Prog. Phys.* **85** 046401

[143] Dombi P, Pápa Z, Vogelsang J, Yalunin S V, Sivis M, Herink G, Schäfer S, Groß P, Ropers C and Lienau C 2020 *Rev. Mod. Phys.* **92** 025003

[144] Shi J, Liang W Y, Raja S S, Sang Y, Zhang X Q, Chen C A, Wang Y, Yang X, Lee Y H, Ahn H and Gwo S 2018 *Laser Photonics Rev.* **12** 1800188

[145] Bernhardt N, Koshelev K, White S J U, Meng K W C, Fröch J E, Kim S, Tran T T, Choi D Y, Kivshar Y and Solntsev A S 2020 *Nano Lett.* **20** 5309

[146] Liu Z, Wang J, Chen B, Wei Y, Liu W and Liu J 2021 *Nano Lett.* **21** 7405

[147] Yuan Q, Fang L, Fang H, Li J, Wang T, Jie W, Zhao J and Gan X 2019 *ACS Photonics* **6** 2252

[148] Wu S, Buckley S, Schaibley J R, Feng L, Yan J, Mandrus D G, Hatami F, Yao W, Vuckovic J, Majumdar A and Xu X 2015 *Nature* **520** 69

[149] Liu Y, Fang H, Rasmita A, Zhou Y, Li J, Yu T, Xiong Q, Zheludev N, Liu J and Gao W 2019 *Sci. Adv.* **5** eaav4506

[150] Dinani H M and Mosallaei H 2023 *Adv. Photonics Res.* **4** 2200207

[151] Hong X, Wang K, Guan C, Han X, Chen Y, Qian S, Xing X, Qiu C W and Lu P 2022 *Nano Lett.* **22** 8860

[152] Huang Z, Luo K, Feng Z, Zhang Z, Li Y, Qiu W, Guan H, Xu Y, Li X and Lu H 2022 *Sci. China Phys. Mech. Astron.* **65** 104211

[153] Vabishchevich P P, Liu S, Sinclair M B, Keeler G A, Peake G M and Brener I 2018 *ACS Photonics* **5** 1685

[154] Kim D, Yu J, Hwang I, Park S, Demmerle F, Boehm G, Amann M C, Belkin M A and Lee J 2020 *Nano Lett.* **20** 8032

[155] Qin J, Huang F, Li X, Deng L, Kang T, Markov A, Yue F, Chen Y, Wen X, Liu S, Xiong Q, Semin S, Rasing T, Modotto D, Morandotti R, Xu J, Duan H and Bi L 2019 *ACS Nano* **13** 1213

[156] Aouani H, Rahmani M, Navarro-Cia M and Maier S A 2014 *Nat. Nanotechnol.* **9** 290

[157] Metzger B, Hentschel M, Schumacher T, Lippitz M, Ye X, Murray C B, Knabe B, Buse K and Giessen H 2014 *Nano Lett.* **14** 2867

[158] Lassiter J B, Chen X, Liu X, Ciracì C, Hoang T B, Larouche S, Oh S H, Mikkelsen M H and Smith D R 2014 *ACS Photonics* **1** 1212

[159] Kruk S, Weismann M, Bykov A Y, Mamonov E A, Kolmychek I A, Murzina T, Panoiu N C, Neshev D N and Kivshar Y S 2015 *ACS Photonics* **2** 1007

[160] Lehr D, Reinhold J, Thiele I, Hartung H, Dietrich K, Menzel C, Pertsch T, Kley E B and Tunnermann A 2015 *Nano Lett.* **15** 1025

[161] Shibanuma T, Grinblat G, Albella P and Maier S A 2017 *Nano Lett.* **17** 2647

[162] Shen Q, Jin W, Yang G, Rodriguez A W and Mikkelsen M H 2020 *ACS Photonics* **7** 901

[163] Wang F, Manjare M, Lemasters R, Li C and Harutyunyan H 2019 *Opt. Lett.* **44** 2787

[164] Liu S, Sinclair M B, Saravi S, Keeler G A, Yang Y, Reno J, Peake G M, Setzpfandt F, Staude I, Pertsch T and Brener I 2016 *Nano Lett.* **16** 5426

[165] Wu X X, Jiang W Y, Wang X F, Zhao L Y, Shi J, Zhang S, Sui X, Chen Z X, Du W N, Shi J W, Liu Q, Zhang Q, Zhang Y and Liu X F 2021 *ACS Nano* **15** 1291

[166] Hu L, Wang B, Guo Y, Du S, Chen J, Li J, Gu C and Wang L 2022 *Adv. Opt. Mater.* **10** 2200193

[167] Wang G, Chernikov A, Glazov M M, Heinz T F, Marie X, Amand T and Urbaszek B 2018 *Rev. Mod. Phys.* **90** 021001

[168] Onga M, Zhang Y, Ideue T and Iwasa Y 2017 *Nat. Mater.* **16** 1193

[169] Mak K F, McGill K L, Park J and McEuen P L 2014 *Science* **344** 1489

[170] Schaibley J R, Yu H, Clark G, Rivera P, Ross J S, Seyler K L, Yao W and Xu X 2016 *Nat. Rev. Mater.* **1** 16055

[171] Liu Y, Gao Y, Zhang S, He J, Yu J and Liu Z 2019 *Nano Res.* **12** 2695

[172] Deng M, Wang X, Chen J, Li Z, Xue M, Zhou Z, Lin F, Zhu X and Fang Z 2021 *Adv. Funct. Mater.* **31** 2010234

[173] Vitale S A, Nezich D, Varghese J O, Kim P, Gedik N, Jarillo-Herrero P, Xiao D and Rothschild M 2018 *Small* **14** 1801483

[174] Krasnok A and Alù A 2018 *Appl. Sci.* **8** 1157

[175] Cao T, Wang G, Han W, Ye H, Zhu C, Shi J, Niu Q, Tan P, Wang E, Liu B and Feng J 2012 *Nat. Commun.* **3** 887

[176] Xiao D, Liu G B, Feng W, Xu X and Yao W 2012 *Phys. Rev. Lett.* **108** 196802

[177] Liu W, Luo C, Tang X, Peng X and Zhong J 2019 *AIP Adv.* **9** 045222

[178] Guo S, Wang Y and Zhang J 2020 *J. Phys. D: Appl. Phys.* **53** 384001

[179] Lee J, Mak K F and Shan J 2016 *Nat. Nanotechnol.* **11** 421

[180] Robert C, Lagarde D, Cadiz F, Wang G, Lassagne B, Amand T, Balocchi A, Renucci P, Tongay S, Urbaszek B and Marie X 2016 *Phys. Rev. B* **93** 205423

[181] Moody G, Dass C K, Hao K, Chen C H, Li L J, Singh A, Tran K, Clark G, Xu X, Berghauser G, Malic E, Knorr A and Li X 2015 *Nat. Commun.* **6** 8315

[182] Guo L, Wu M, Cao T, Monahan D M, Lee Y H, Louie S G and Fleming G R 2018 *Nat. Phys.* **15** 228

[183] Yang M, Robert C, Lu Z, Van Tuan D, Smirnov D, Marie X and Dery H 2020 *Phys. Rev. B* **101** 115307

[184] Norden T, Zhao C, Zhang P, Sabirianov R, Petrou A and Zeng H 2019 *Nat. Commun.* **10** 4163

[185] Singh A, Tran K, Kolarczik M, Seifert J, Wang Y, Hao K, Pleskot D, Gabor N M, Helmrich S, Owschimikow N, Woggon U and Li X 2016 *Phys. Rev. Lett.* **117** 257402

[186] Novotny L and Hecht B 2012 *Principles of Nano-Optics* (2nd edn.) (Cambridge: Cambridge University Press)

[187] Zu S, Han T, Jiang M, Liu Z, Jiang Q, Lin F, Zhu X and Fang Z 2019 *Nano Lett.* **19** 775

[188] Zhou H L, Zhang X Y, Xue X M, Yang Y, Wang S J, Su D, Yang Z R, Wang Y F, Song Y, Wu J, Wu W and Zhang T 2022 *Nano Lett.* **22** 6923

[189] Liu S, Chen S, Wen S and Luo H 2022 *Opto-Electron. Sci.* **1** 220007

[190] Bliokh K Y, Rodríguez-Fortuño F J, Nori F and Zayats A V 2015 *Nat. Photon.* **9** 796

[191] Petersen J, Volz J and Rauschenbeutel A 2014 *Science* **346** 67

[192] Rodríguez-Fortuño F J, Marino G, Ginzburg P, O'Connor D, Martínez A, Wurtz G A and Zayats A V 2013 *Science* **340** 328

[193] Gong S H, Alpeggiani F, Sciacca B, Garnett E C and Kuipers L 2018 *Science* **359** 443

[194] Gong S H, Komen I, Alpeggiani F and Kuipers L 2020 *Nano Lett.* **20** 4410

[195] Sun L, Wang C Y, Krasnok A, Choi J, Shi J, Gomez-Diaz J S, Zepeda A, Gwo S, Shih C K, Alù A and Li X 2019 *Nat. Photonics* **13** 180

[196] Chen Y, Qian S, Wang K, Xing X, Wee A, Loh K P, Wang B, Wu D, Chu J, Alù A, Lu P and Qiu C W 2022 *Nat. Nanotechnol.* **17** 1178

[197] Streltsov A, Adesso G and Plenio M B 2017 *Rev. Mod. Phys.* **89** 041003

[198] Zhou Y, Scuri G, Wild D S, High A A, Dibos A, Jauregui L A, Shu C, De Greve K, Pistunova K, Joe A Y, Taniguchi T, Watanabe K, Kim P, Lukin M D and Park H 2017 *Nat. Nanotechnol.* **12** 856

[199] Jha P K, Shitrit N, Ren X, Wang Y and Zhang X 2018 *Phys. Rev. Lett.* **121** 116102

[200] Hu G, Hong X, Wang K, Wu J, Xu H X, Zhao W, Liu W, Zhang S, Garcia-Vidal F, Wang B, Lu P and Qiu C W 2019 *Nat. Photonics* **13** 467

[201] Chervy T, Azzini S, Lorchat E, Wang S, Gorodetski Y, Hutchison J A, Berciaud S, Ebbesen T W and Genet C 2018 *ACS Photonics* **5** 1281

[202] Li Z, Li Y, Han T, Wang X, Yu Y, Tay B, Liu Z and Fang Z 2017 *ACS Nano* **11** 1165

[203] Deng M, Li Z, Rong X, Luo Y, Li B, Zheng L, Wang X, Lin F, Meixner A J, Braun K, Zhu X and Fang Z 2020 *Small* **16** 2003539

[204] Li Z, Liu C, Rong X, Luo Y, Cheng H, Zheng L, Lin F, Shen B, Gong Y, Zhang S and Fang Z 2018 *Adv. Mater.* **30** 1801908

[205] Lin H T, Chang C Y, Cheng P J, Li M Y, Cheng C C, Chang S W, Li L L J, Chu C W, Wei P K and Shih M H 2018 *ACS Appl. Mater. Interfaces* **10** 15996

[206] Guddala S, Bushati R, Li M, Khanikaev A B and Menon V M 2019 *Opt. Mater. Express* **9** 536

[207] Chen H, Liu M, Xu L and Neshev D N 2018 *Beilstein J. Nanotechnol.* **9** 780

[208] Wen T, Zhang W, Liu S, Hu A, Zhao J, Ye Y, Chen Y, Qiu C W, Gong Q and Lu G 2020 *Sci. Adv.* **6** eaao0019

[209] Altewischer E, Van Exter M P and Woerdman J P 2002 *Nature* **418** 304

[210] Tan S F, Wu L, Yang J K W, Bai P, Bosman M and Nijhuis C A 2014 *Science* **343** 1496

[211] Dheur M C, Devaux E, Ebbesen T W, Baron A, Rodier J C, Hugonin J P, Lalanne P, Greffet J J, Messin G and Marquier F 2016 *Sci. Adv.* **2** e1501574

[212] Iwanaga M, Mano T and Ikeda N 2017 *ACS Photonics* **5** 897

[213] Tran T T, Wang D, Xu Z Q, Yang A, Toth M, Odom T W and Aharonovich I 2017 *Nano Lett.* **17** 2634

[214] Wu C, Kumar S, Kan Y, Komisar D, Wang Z, Bozhevolnyi S I and Ding F 2022 *Sci. Adv.* **8** eabk3075

[215] Li L, Liu Z, Ren X, Wang S, Su V C, Chen M K, Chu C H, Kuo H Y, Liu B, Zang W, Guo G, Zhang L, Wang Z, Zhu S and Tsai D P 2020 *Science* **368** 1487

[216] Marino G, Solntsev A S, Xu L, Gili V F, Carletti L, Poddubny A N, Rahmani M, Smirnova D A, Chen H, Lemaître A, Zhang G, Zayats A V, De Angelis C, Leo G, Sukhorukov A A and Neshev D N 2019 *Optica* **6** 1416

[217] Jin B, Mishra D and Argyropoulos C 2021 *Nanoscale* **13** 19903

[218] Zhang J, Ma J, Parry M, Cai M, Camacho-Morales R, Xu L, Neshev D N and Sukhorukov A A 2022 *Sci. Adv.* **8** eabq4240

[219] Santiago-Cruz T, Gennaro S D, Mitrofanov O, Addamane S, Reno J, Brener I and Chekhova M V 2022 *Science* **377** 991

[220] Wang Y, Jöns K D and Sun Z 2021 *Appl. Phys. Rev.* **8** 011314

[221] Georgi P, Massaro M, Luo K H, Sain B, Montaut N, Herrmann H, Weiss T, Li G, Silberhorn C and Zentgraf T 2019 *Light Sci. Appl.* **8** 70

[222] Brida G, Genovese M and Ruo B I 2010 *Nat. Photonics* **4** 227

[223] Wang K, Titchener J G, Kruk S S, Xu L, Chung H P, Parry M, Kravchenko I I, Chen Y H, Solntsev A S, Kivshar Y S, Neshev D N and Sukhorukov A A 2018 *Science* **361** 1104

[224] Stav T, Faerman A, Maguid E, Oren D, Kleiner V, Hasman E and Segev M 2018 *Science* **361** 1101

[225] Kan Y, Andersen S K H, Ding F, Kumar S, Zhao C and Bozhevolnyi S I 2020 *Adv. Mater.* **32** 1907832

[226] Ma Y, Zhao H, Liu N, Gao Z, Mohajerani S S, Xiao L, Hone J, Feng L and Strauf S 2022 *Optica* **9** 953

[227] Altuzarra C, Lyons A, Yuan G, Simpson C, Roger T, Ben-Benjamin J S and Faccio D 2019 *Phys. Rev. A* **99** 020101

[228] Solntsev A S, Agarwal G S and Kivshar Y S 2021 *Nat. Photonics* **15** 327

[229] Kan Y and Bozhevolnyi S I 2023 *Adv. Opt. Mater.* **11** 2202759

[230] Ates S, Ulrich S M, Ulhaq A, Reitzenstein S, Löffler A, Höfling S, Forchel A and Michler P 2009 *Nat. Photonics* **3** 724
[231] Kwiat P G, Mattle K, Weinfurter H, Zeilinger A, Sergienko A V and Shih Y 1995 *Phys. Rev. Lett.* **75** 4337
[232] Schneeloch J, Knarr S H, Bogorin D F, Levangie M L, Tison C C, Frank R, Howland G A, Fanto M L and Alsing P M 2019 *J. Opt.* **21** 043501
[233] Main P B, Mosley P J and Gorbach A V 2019 *Phys. Rev. A* **100** 053815
[234] Introini V, Steel M J, Sipe J E, Helt L G and Liscidini M 2020 *Opt. Lett.* **45** 1244
[235] Okoth C, Cavanna A, Santiago-Cruz T and Chekhova M V 2019 *Phys. Rev. Lett.* **123** 263602
[236] Carletti L, Koshelev K, De Angelis C and Kivshar Y 2018 *Phys. Rev. Lett.* **121** 033903
[237] Kuo P S, Bravo-Abad J and Solomon G S 2014 *Nat. Commun.* **5** 3109
[238] Hsu C W, Zhen B, Stone A D, Joannopoulos J D and Soljačić M 2016 *Nat. Rev. Mater.* **1** 16048
[239] Lin H, Zhang Z, Zhang H, Lin K T, Wen X, Liang Y, Fu Y, Lau A K T, Ma T, Qiu C W and Jia B 2022 *Chem. Rev.* **122** 15204
[240] Carletti L, Kruk S S, Bogdanov A A, De Angelis C and Kivshar Y 2019 *Phys. Rev. Res.* **1** 023016
[241] Shcherbakov M R, Zhang H, Tripepi M, Sartorello G, Talisa N, AlShafey A, Fan Z, Twardowski J, Krivitsky L A, Kuznetsov A I, Chowdhury E and Shvets G 2021 *Nat. Commun.* **12** 4185
[242] Zeng Z, Sun X, Zhang D, Zheng W, Fan X, He M, Xu T, Sun L, Wang X and Pan A 2019 *Adv. Funct. Mater.* **29** 1806874
[243] Fan X, Ji Z, Fei R, Zheng W, Liu W, Zhu X, Chen S, Yang L, Liu H, Pan A and Agarwal R 2020 *Nano Lett.* **20** 2667
[244] Shan Y, Li Y, Huang D, Tong Q, Yao W, Liu W T and Wu S 2018 *Sci. Adv.* **4** eaat0074
[245] Liu F, Wu W, Bai Y, Chae S H, Li Q, Wang J, Hone J and Zhu X Y 2020 *Science* **367** 903
[246] Trovatello C, Marini A, Xu X, Lee C, Liu F, Curreli N, Manzoni C, Dal Conte S, Yao K, Ciattoni A, Hone J, Zhu X, Schuck P J and Cerullo G 2020 *Nat. Photonics* **15** 6
[247] Guo Q, Qi X Z, Zhang L, Gao M, Hu S, Zhou W, Zang W, Zhao X, Wang J, Yan B, Xu M, Wu Y K, Eda G, Xiao Z, Yang S A, Gou H, Feng Y P, Guo G C, Zhou W, Ren X F, Qiu C W, Pennycook S J and Wee A T S 2023 *Nature* **613** 53
[248] Le C T, Kim J, Ullah F, Nguyen A D, Tran T N N, Le T E, Chung K H, Cheong H, Jang J I and Kim Y S 2020 *ACS Nano* **14** 4366